Superfluidity in neutron-star crusts

Nicolas Chamel

Institut d'Astronomie et d'Astrophysique
Université Libre de Bruxelles, Belgique

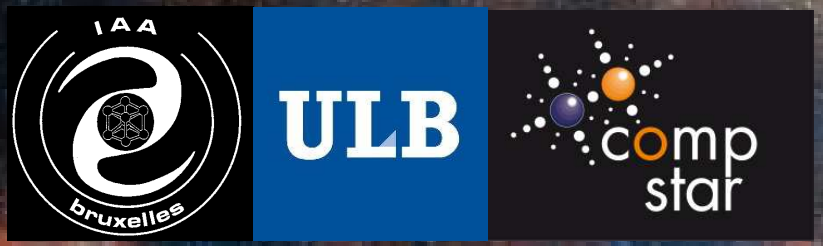

INT, Seattle, May 2011

Why studying superfluidity in neutron stars?

Neutron stars are by nature quantum systems: they contain highly degenerate matter which can therefore exhibit various phenomena observed in condensed matter physics like superfluidity.

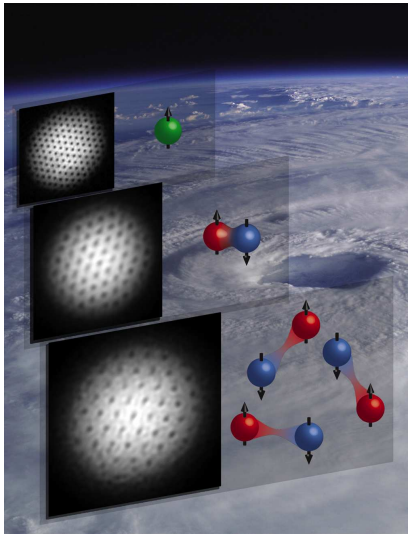

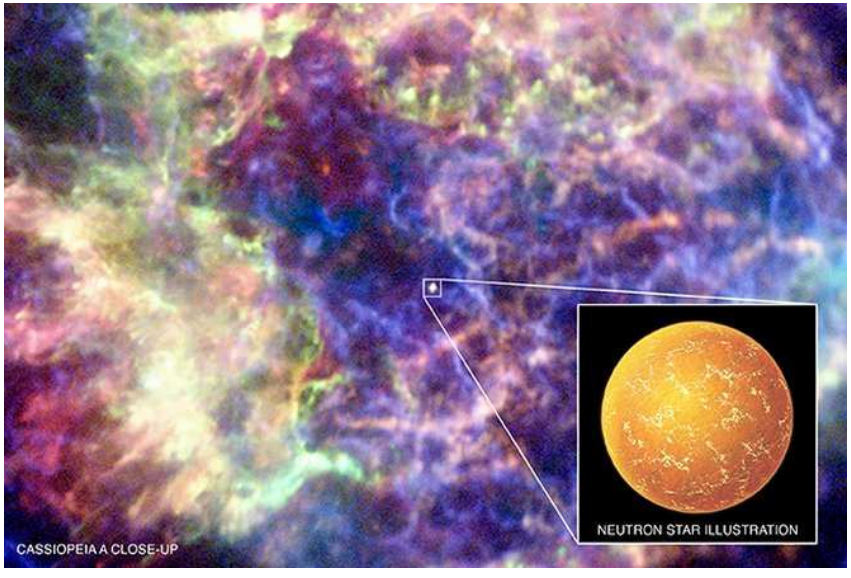

Cassiopeia A (NASA)

Superfluidity affects the evolution of neutron stars: pulsar glitches, pulsations, precession, cooling, magnetic field...

Are electrons in neutron stars superconducting?

The surface layers of non-accreting neutron stars are mostly composed of ordinary iron which is not superconducting.

It was found in 2001 (Shimizu et al., Nature 412, 316) that iron under pressure can become superconducting at densities $\rho \simeq 8.2$ g.cm^{-3} with $T_{ce} \simeq 2$ K.

But T_{ce} is much smaller than the temperature in neutron stars.

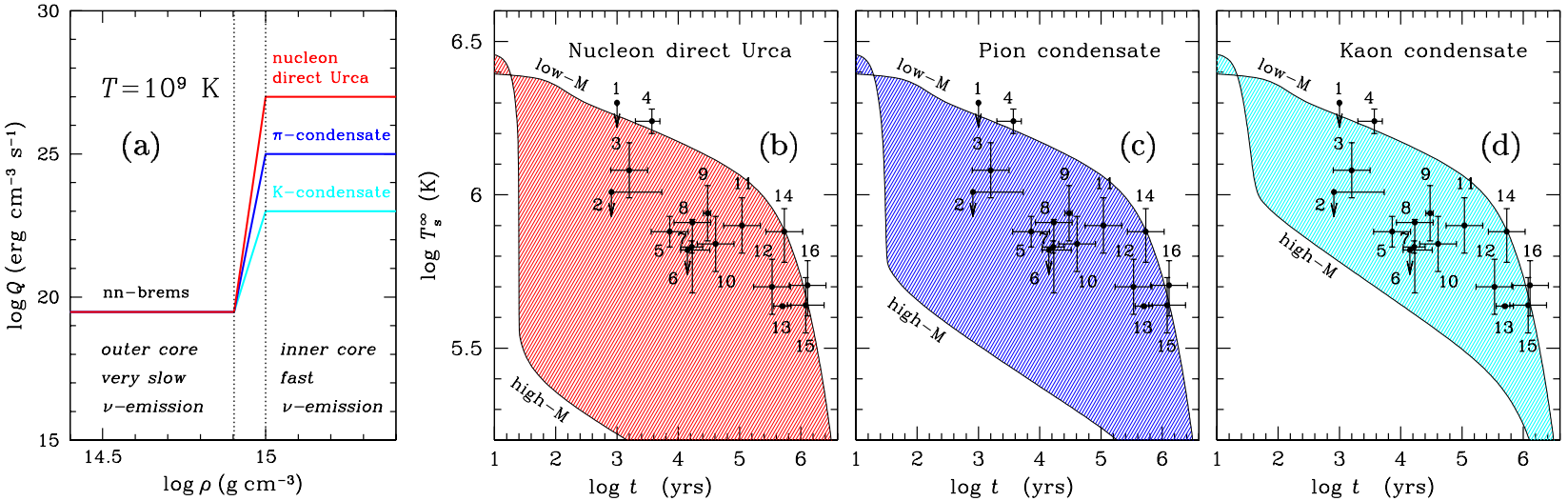

Yakovlev et al, proceedings (2007), arXiv:0710.2047

Are electrons in neutron stars superconducting?

In the deeper layers of neutron stars at densities $\rho \gtrsim 10^4$ gcm^{-3}, **atoms are fully ionised by the pressure**.

The critical temperature of a uniform non-relativistic electron gas (jelium) is given by ($T_{\rm pi}$ is the plasma temperature)

$$T_{\rm ce} = T_{\rm pi} \exp\left(-8\hbar v_{\rm Fe}/\pi e^2\right) \Rightarrow T_{\rm ce} \propto \exp(-\zeta(\rho/\rho_{\rm ord})^{1/3})$$

with $\rho_{\rm ord} = m_{\rm u}/(4\pi a_0^3/3)$. At densities above $\sim 10^6$ g.cm^{-3}, electrons become relativistic $v_{\rm Fe} \sim c$ so that ($\alpha = e^2/\hbar c \simeq 1/137$)

$$T_{\rm ce} = T_{\rm pi} \exp\left(-8/\pi\alpha\right) \sim 0$$

Ginzburg, J. Stat. Phys. 1(1969),3.

Electrons in neutron stars are not superconducting.

Nuclear superfluidity in neutron stars

The BCS theory was applied to nuclei by Bohr, Mottelson, Pines and Belyaev
Phys. Rev. 110, 936 (1958).
Mat.-Fys. Medd. K. Dan. Vid. Selsk. 31 , 1 (1959).

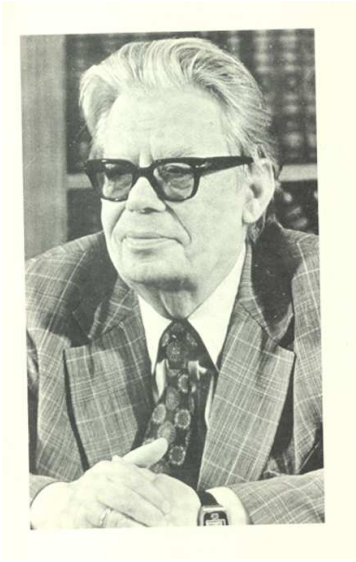

N.N. Bogoliubov, who developed a microscopic theory of superfluidity and superconductivity, was the first to explore its application to nuclear matter.
Dokl. Ak. nauk SSSR 119, 52 (1958).

Superfluidity in neutron stars was suggested long ago (before the actual discovery of neutron stars) by Migdal in 1959. It was first studied by Ginzburg and Kirzhnits in 1964.
Ginzburg and Kirzhnits, Zh. Eksp. Teor. Fiz. 47, 2006, (1964).

Superfluidity and superconductivity in neutron stars

In spite of their names, neutron stars are not only made of neutrons! As a consequence, they could contain various kinds of superfluids and superconductors.

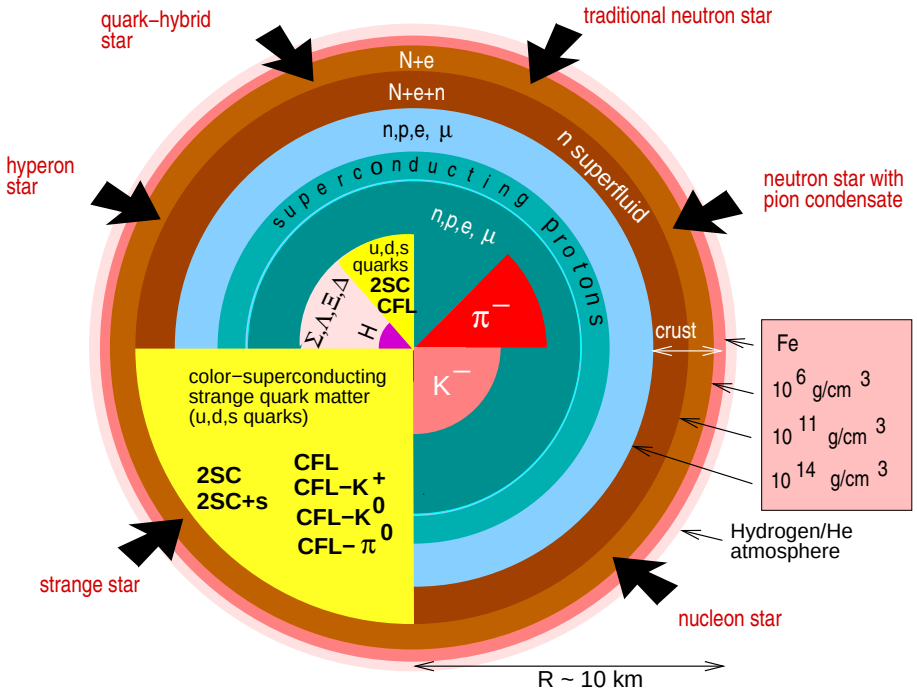

picture from F. Weber

Neutron stars are expected to contain at least a neutron superfluid in their crust.

Superfluidity in neutron-star crusts

Most microscopic calculations have been performed in uniform neutron matter.

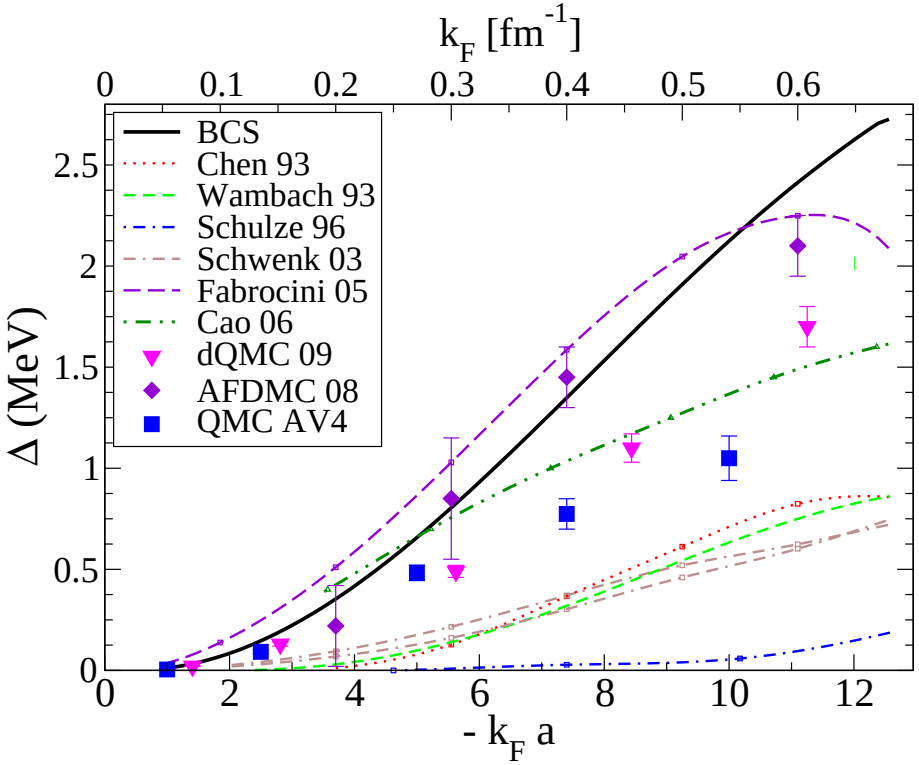

Microscopic calculations using different methods predict different density dependence of the $^1S_0$ pairing gaps.

Gezerlis & Carlson, Phys. Rev. C 81, 025803 (2010).

Is the neutron superfluid in the crust really uniform? What is the effect of the nuclei?

Nuclear energy density functional theory in a nut shell

The nuclear energy density functional theory allows for a **tractable and consistent** treatment of nuclear matter, atomic nuclei and neutron-star crusts.

The energy of a lump of matter is expressed as ($q = n, p$)

$$E = \int \mathcal{E}\Big[\rho_q(\boldsymbol{r}), \boldsymbol{\nabla}\rho_q(\boldsymbol{r}), \tau_q(\boldsymbol{r}), \boldsymbol{J}_q(\boldsymbol{r}), \tilde{\rho}_q(\boldsymbol{r})\Big]\, \mathrm{d}^3\boldsymbol{r}$$

where $\rho_q(\boldsymbol{r})$, $\tau_q(\boldsymbol{r})$... are functionals of $\varphi_{1k}^{(q)}(r)$ and $\varphi_{2k}^{(q)}(r)$

$$\begin{pmatrix} h_q(r) - \lambda_q & \Delta_q(r) \\ \Delta_q(r) & -h_q(r) + \lambda_q \end{pmatrix} \begin{pmatrix} \varphi_{1k}^{(q)}(r) \\ \varphi_{2k}^{(q)}(r) \end{pmatrix} = E_k^{(q)} \begin{pmatrix} \varphi_{1k}^{(q)}(r) \\ \varphi_{2k}^{(q)}(r) \end{pmatrix}$$

$$h_q \equiv -\boldsymbol{\nabla} \cdot \frac{\delta E}{\delta \tau_q} \boldsymbol{\nabla} + \frac{\delta E}{\delta \rho_q} - \mathrm{i} \frac{\delta E}{\delta \boldsymbol{J}_q} \cdot \boldsymbol{\nabla} \times \boldsymbol{\sigma}\,, \qquad \Delta_q \equiv \frac{\delta E}{\delta \tilde{\rho}_q}$$

Effective nuclear energy density functional

- In principle, one can construct the nuclear functional from realistic nucleon-nucleon forces (i.e. fitted to experimental nucleon-nucleon phase shifts) using many-body methods

$$\mathcal{E} = \frac{\hbar^2}{2M}(\tau_n + \tau_p) + A(\rho_n, \rho_p) + B(\rho_n, \rho_p)\tau_n + B(\rho_p, \rho_n)\tau_p$$

$$+C(\rho_n, \rho_p)(\nabla\rho_n)^2 + C(\rho_p, \rho_n)(\nabla\rho_p)^2 + D(\rho_n, \rho_p)(\nabla\rho_n)\cdot(\nabla\rho_p)$$

+ Coulomb, spin-orbit and pairing

Drut et al.,Prog.Part.Nucl.Phys.64(2010)120.

- But difficult task so in practice, we use phenomenological (Skyrme) functionals

Bender et al.,Rev.Mod.Phys.75, 121 (2003).

Phenomenological corrections for atomic nuclei

For atomic nuclei, we add the following corrections:

$$E_{\mathrm{corr}} = E_W + E_{\mathrm{coll}}$$

- Wigner energy

$$E_W = V_W \exp\left\{-\lambda\left(\frac{N-Z}{A}\right)^2\right\} + V'_W|N-Z|\exp\left\{-\left(\frac{A}{A_0}\right)^2\right\}$$

- rotational and vibrational spurious collective energy

$$E_{\mathrm{coll}} = E_{\mathrm{rot}}^{\mathrm{crank}}\left\{b\ \tanh(c|\beta_2|) + d|\beta_2|\ \exp\{-I(|\beta_2| - \beta_2^0)^2\}\right\}$$

Construction of the functional

Experimental data:

- 2149 measured nuclear masses with $Z, N \geq 8$
- compressibility $230 \leq K_v \leq 250$ MeV
- charge radius of ^{208}Pb, $R_c = 5.501 \pm 0.001$ fm

N-body calculations with realistic forces:

- isoscalar effective mass $M_s^*/M = 0.8$
- equation of state of pure neutron matter
- $^1S_0$ pairing gaps in symmetric and neutron matter
- Landau parameters (stability against spurious instabilities)

Chamel, Goriely, Pearson, Phys.Rev.C80,065804 (2009).
Chamel&Goriely, Phys.Rev.C82, 045804 (2010)

With these constraints, the functional is well suited for describing neutron-star crusts.

Empirical pairing energy density functionals

$$\mathcal{E}_{\text{pair}} = \frac{1}{4} \sum_{q=n,p} v^{\pi q}[\rho_n, \rho_p] \tilde{\rho}_q^2$$

$$v^{\pi q}[\rho_n, \rho_p] = V_{\pi q}^{\Lambda} \left(1 - \eta_q \left(\frac{\rho_n + \rho_p}{\rho_0} \right)^{\alpha_q} \right)$$

Drawbacks

- not enough flexibility to fit realistic pairing gaps in infinite nuclear matter and in finite nuclei ($\Rightarrow$ isospin dependence)
- the global fit to nuclear masses would be computationally very expensive

Microscopically deduced pairing functional

Assumptions:

- $v^{\pi\, q}[\rho_n, \rho_p] = v^{\pi\, q}[\rho_q]$ depends *only* on ρ_q
  Duguet, Phys. Rev. C 69 (2004) 054317.
- isospin charge symmetry $v^{\pi\, n} = v^{\pi\, p} = v^{\pi}$
- $v^{\pi}[\rho_q]$ is the *locally* the same as in infinite nuclear matter with density ρ_q

$v^{\pi}[\rho_q] = v^{\pi}[\Delta_q(\rho_q)]$ constructed so as to reproduce *exactly* a given pairing gap $\Delta_q(\rho_q)$ in infinite homogeneous matter by solving *directly* the HFB equations

Chamel, Goriely, Pearson, Nucl. Phys.A812,72 (2008).

Pairing in nuclei and in nuclear matter

Inverting the HFB equations yields

$$v^{\pi}[\rho_q] = -8\pi^2 \left(\frac{\hbar^2}{2M_q^*}\right)^{3/2} \left(\int_0^{\mu_q+\varepsilon_\Lambda} \mathrm{d}\varepsilon \frac{\sqrt{\varepsilon}}{\sqrt{(\varepsilon-\mu_q)^2+\Delta_q(\rho_q)^2}}\right)^{-1}$$

$$\mu_q = \frac{\hbar^2}{2M_q^*}(3\pi^2\rho_q)^{2/3}$$

Cutoff prescription: s.p. energy cutoff ε_Λ above the Fermi level

This procedure provides a one-to-one correspondence between the pairing strength in finite nuclei and the $^1S_0$ pairing gap in infinite nuclear matter.

Analytical expression of the pairing strength

In the "weak-coupling approximation" $\Delta_q \ll \mu_q$ and $\Delta_q \ll \varepsilon_\Lambda$

$$v^\pi[\rho_q] = -\frac{8\pi^2}{I_q(\rho_q)} \left(\frac{\hbar^2}{2M_q^*(\rho_q)} \right)^{3/2}$$

$$I_q = \sqrt{\mu_q} \left[2 \log \left(\frac{2\mu_q}{\Delta_q} \right) + \Lambda \left(\frac{\varepsilon_\Lambda}{\mu_q} \right) \right]$$

$$\Lambda(x) = \log(16x) + 2\sqrt{1+x} - 2 \log \left(1 + \sqrt{1+x} \right) - 4$$

Chamel, Phys. Rev. C 82, 014313 (2010)

- **exact fit** of the given gap function $\Delta_q(\rho_q)$
- **no free parameters**
- **automatic renormalization** of the pairing strength with ε_Λ

Pairing gaps from contact interactions

The weak-coupling approximation can also be used to determine the pairing gap of a Fermi gas interacting with a contact force

$$\Delta = 2\mu \exp\left(\frac{2}{g(\mu)v^{\pi}_{\rm reg}}\right)$$

μ is the chemical potential, $g(\mu)$ is the density of states and v^{π}_{Λ} is a regularized interaction

$$\frac{1}{v^{\pi}_{\rm reg}} = \frac{1}{v^{\pi}} + \frac{1}{v^{\pi}_{\Lambda}}$$

$$v^{\pi}_{\Lambda} = \frac{4}{g(\mu)\Lambda(\varepsilon_{\Lambda}/\mu)}$$

Accuracy of the weak-coupling approximation

This approximation remains very accurate at low densities because the s.p. density of states is not replaced by a constant as usually done.

symmetric nuclear matter

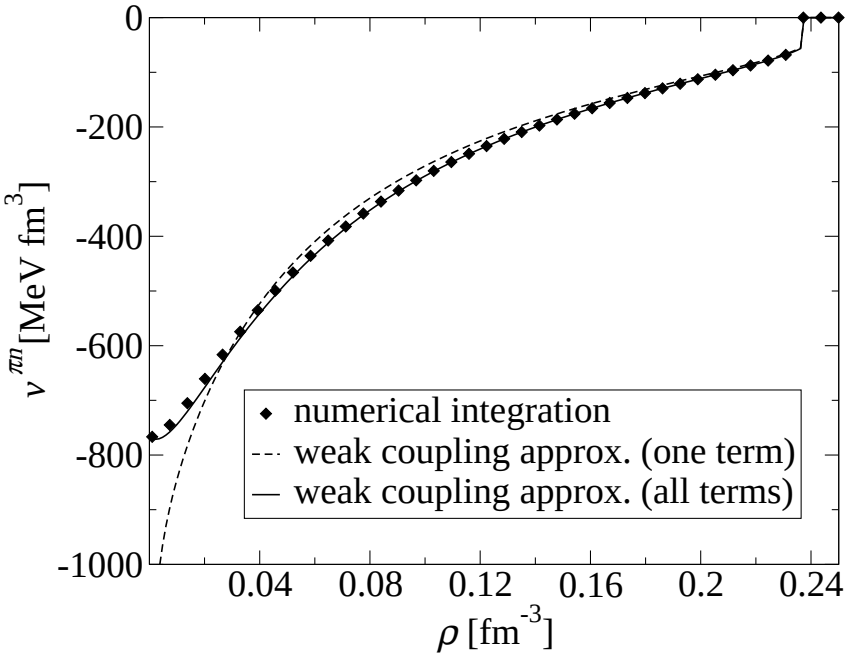

neutron matter

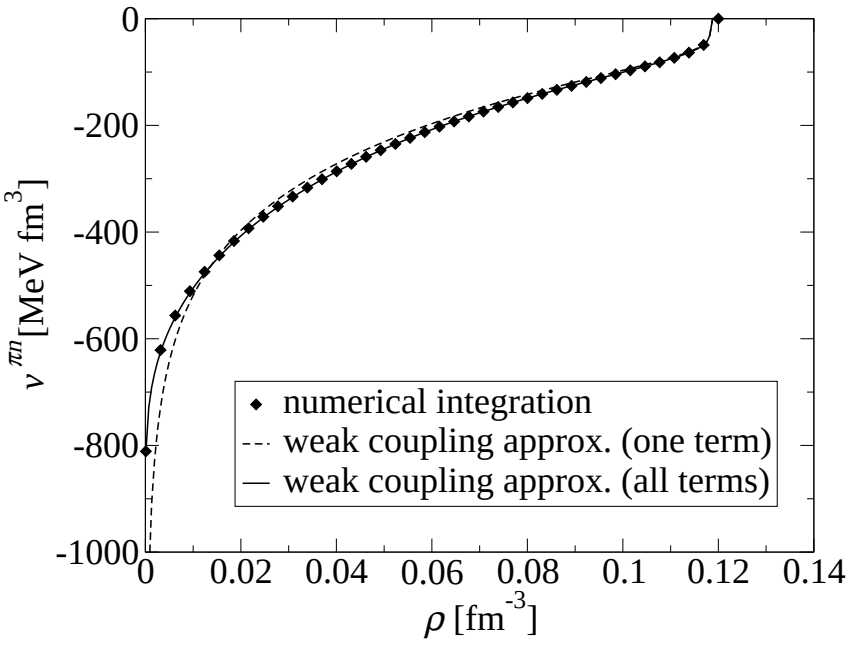

Chamel, Phys. Rev. C 82, 014313 (2010)

Pairing in dilute neutron matter

At very low densities, the pairing gap is given by

$$\Delta_n = \left(\frac{2}{e}\right)^{7/3} \mu_n \exp\left(\frac{\pi}{2k_F a_{nn}}\right)$$

Gorkov&Melik-Barkhudarov, Sov. Phys. JETP, 13, 1018, (1961).

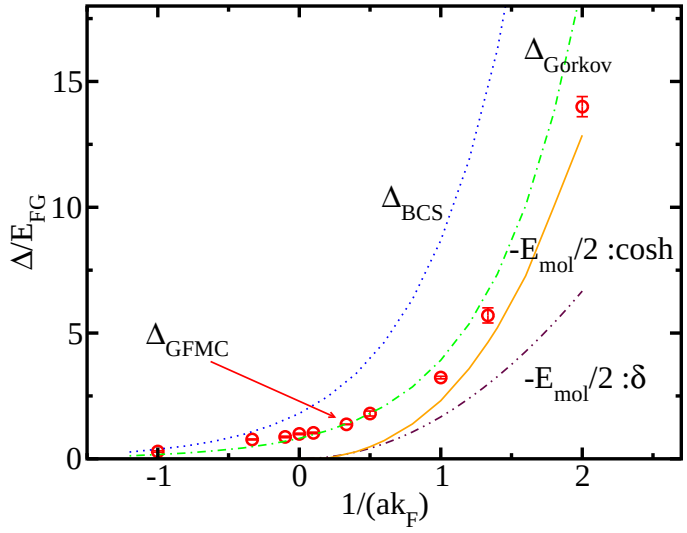

Chang et al. Phys.Rev.A70, 043602 (2004).

$$\Rightarrow v^{\pi}[\rho_n] = -\frac{8\pi^2}{I_n(\rho_n)}\left(\frac{\hbar^2}{2M_n^*(\rho_n)}\right)^{3/2}$$

$$I_n = \sqrt{\mu_n}\left[\frac{14}{3} - \frac{8}{3}\log 2 - \left(\frac{\pi}{k_F a_{nn}}\right) + \Lambda\left(\frac{\varepsilon\Lambda}{\mu_n}\right)\right]$$

Pairing cutoff and experimental phase shifts

In the limit of vanishing density, the pairing strength

$$v^{\pi}[\rho_q \to 0] = -\frac{4\pi^2}{\sqrt{\varepsilon_\Lambda}} \left(\frac{\hbar^2}{2M_q} \right)^{3/2}$$

should coincide with the bare force in the $^1S_0$ channel.

A fit to the **experimental $^1S_0$ NN phase shifts** yields $\varepsilon_\Lambda \sim 7 - 8$ MeV.
Esbensen et al., Phys. Rev. C 56, 3054 (1997).

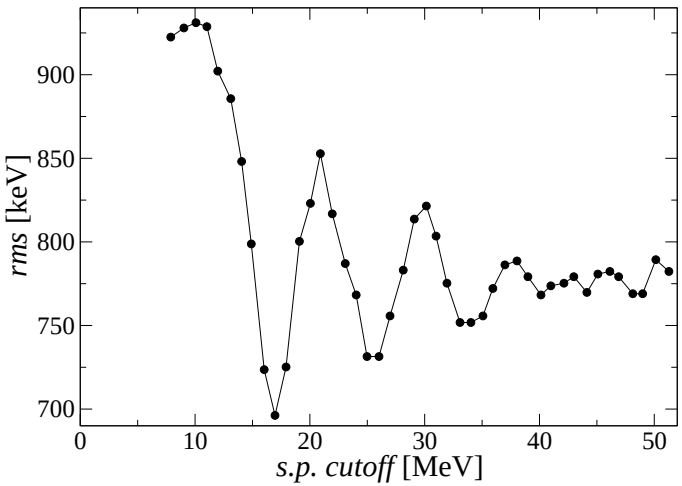

On the other hand, a better mass fit can be obtained with $\varepsilon_\Lambda \sim 16$ MeV while convergence is achieved for $\varepsilon_\Lambda \gtrsim 40$ MeV.
Goriely et al., Nucl.Phys.A773(2006),279.

Choice of the pairing gap

Fit the $^1S_0$ pairing gap obtained with realistic NN potentials at the BCS level (no medium effects)

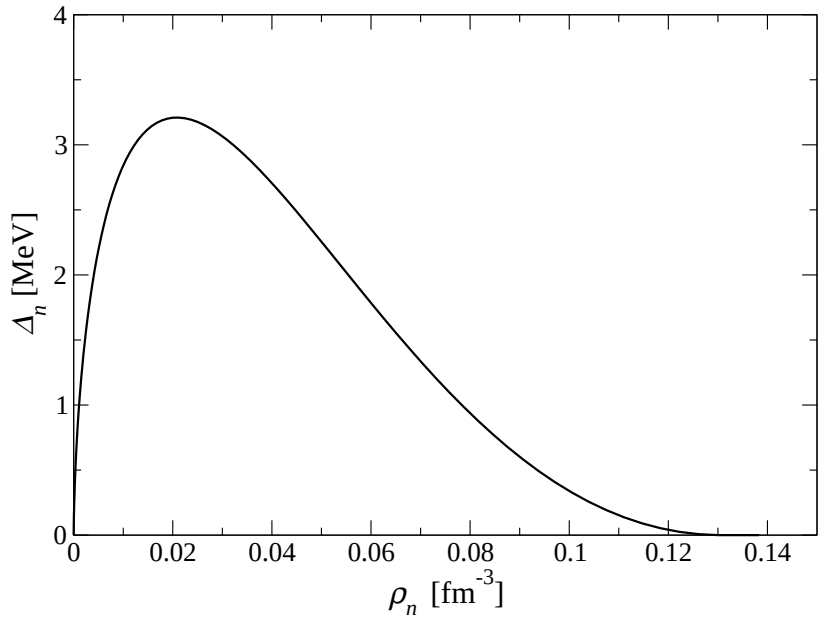

Pairing gap obtained with Argonne V_{14} potential

- $\Delta_n(\rho_n)$ essentially independent of the NN potential
- $\Delta_n(\rho_n)$ completely determined by experimental $^1S_0$ nn phase shifts

Dean&Hjorth-Jensen,Rev.Mod.Phys.75(2003)607.

Neutron vs proton pairing

- Because of possible **charge symmetry breaking effects**, proton and neutron pairing strengths may not be equal

$$v^{\pi\, n}[\rho] \neq v^{\pi\, p}[\rho]$$

- The neglect of **polarization effects in odd nuclei** (equal filling approximation) is corrected by “staggered” pairing

$\Rightarrow$ we introduce renormalization factors $f_q^{\pm}$ ($f_n^{+} \equiv 1$ by definition)

$$v^{\pi\, n}[\rho_n] = f_n^{\pm} v^{\pi}[\rho_n]$$

$$v^{\pi\, p}[\rho_p] = f_p^{\pm} v^{\pi}[\rho_p]$$

Neutron vs proton pairing

What comes out of the global mass fit?

f_n^+	1.00
f_n^-	1.06
f_p^+	0.99
f_p^-	1.05

$\Rightarrow$ neutron and proton pairing strengths are effectively equal $f_n^-/f_n^+ \simeq f_p^-/f_p^+$

$\Rightarrow$ the pairing strength is larger for odd nuclei $f_q^- > f_q^+$

This is in agreement with a recent analysis by Bertsch et al. *Phys.Rev.C79(2009),034306*

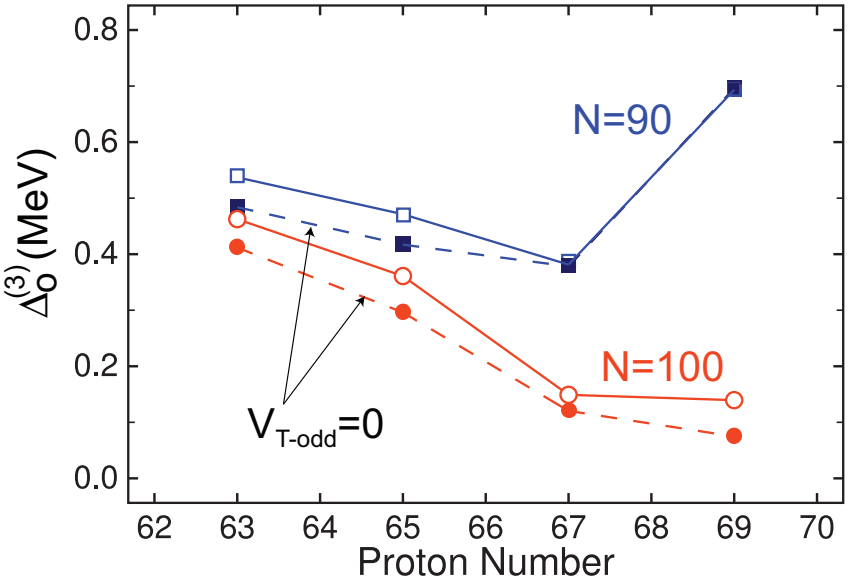

$^1S_0$ pairing gap in neutron matter

This new mass model yields a much more realistic gap than our previous mass models!

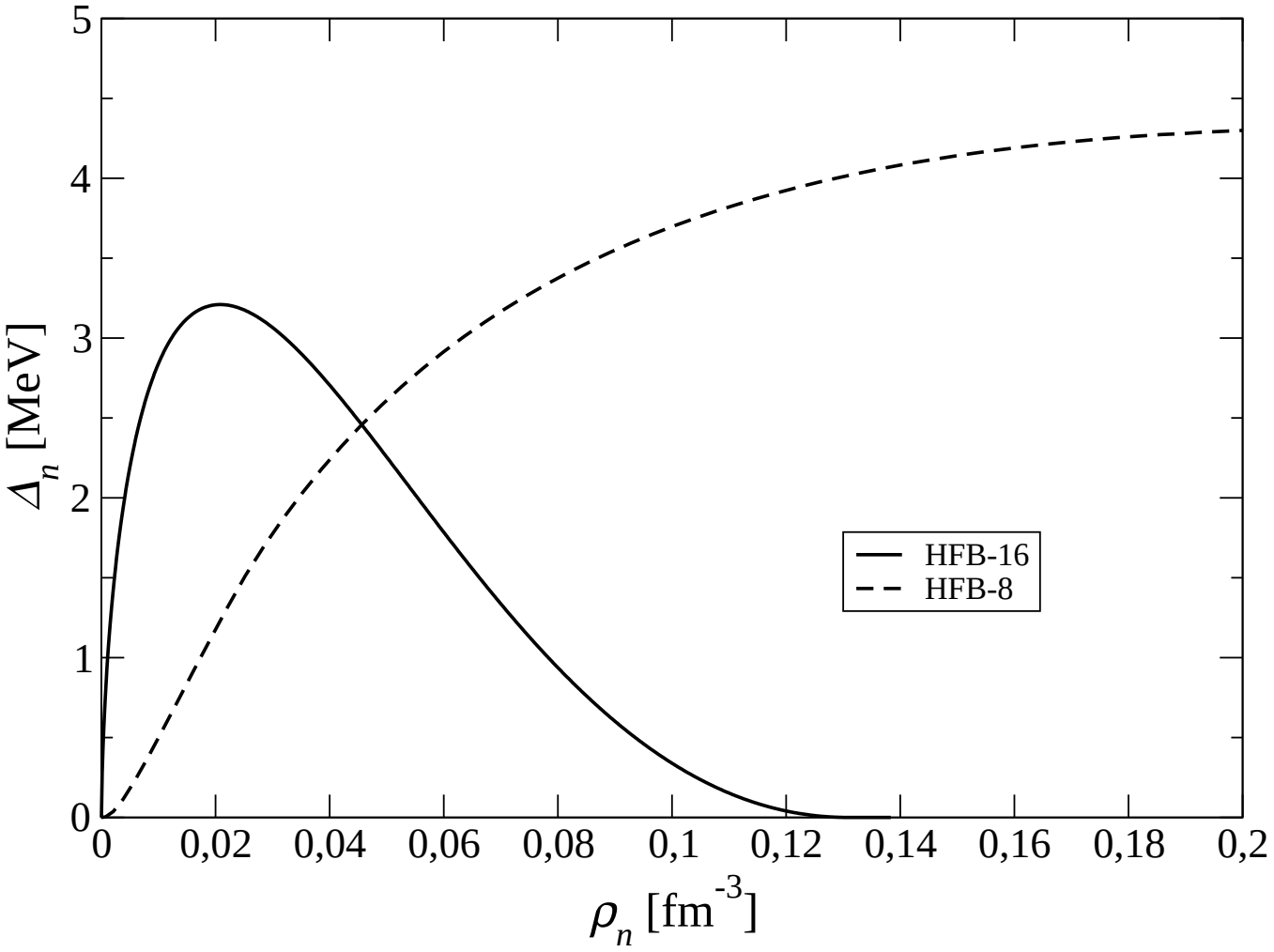

Neutron-matter equation of state at subsaturation densities

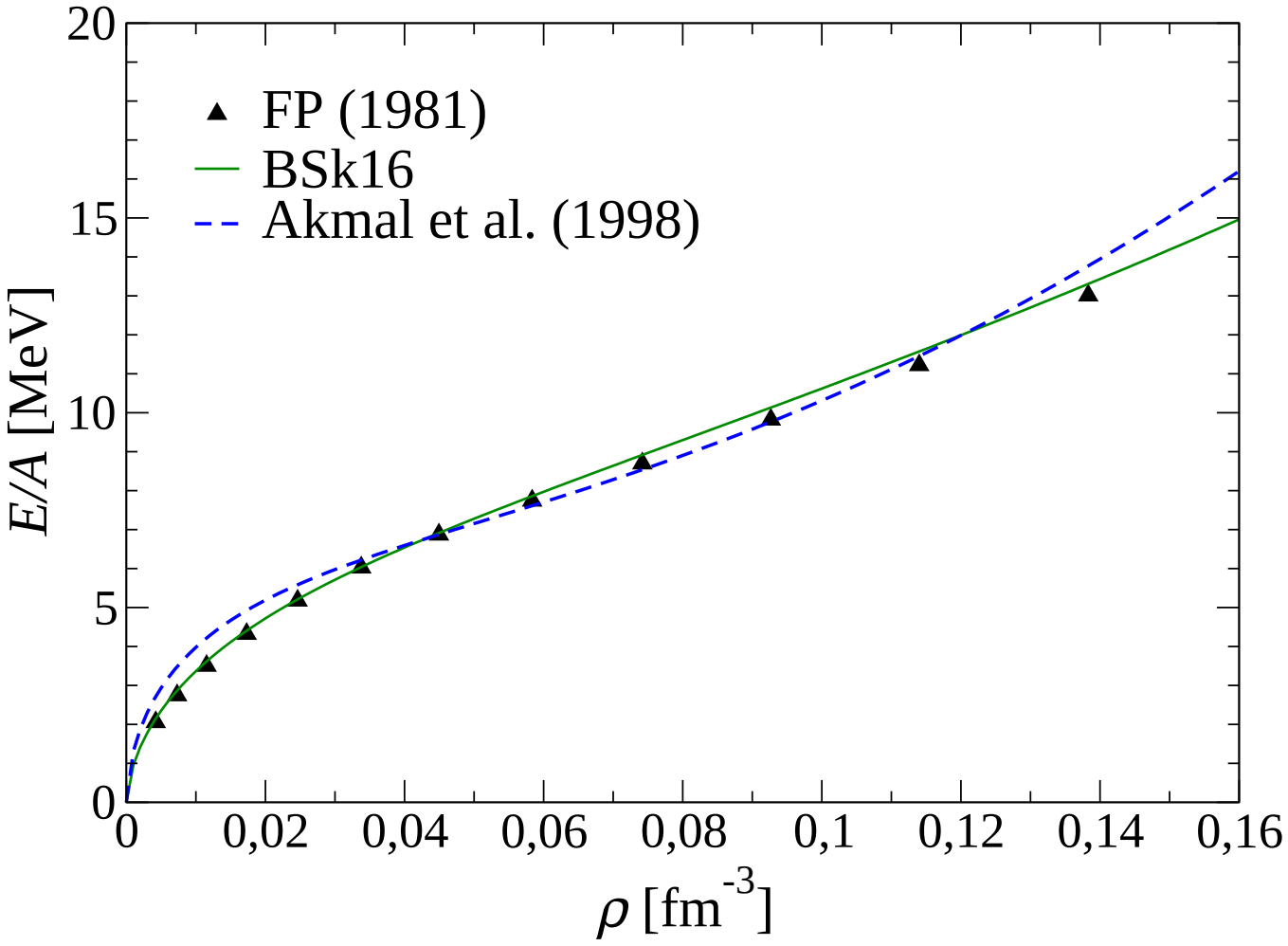

Dilute neutron-matter equation of state

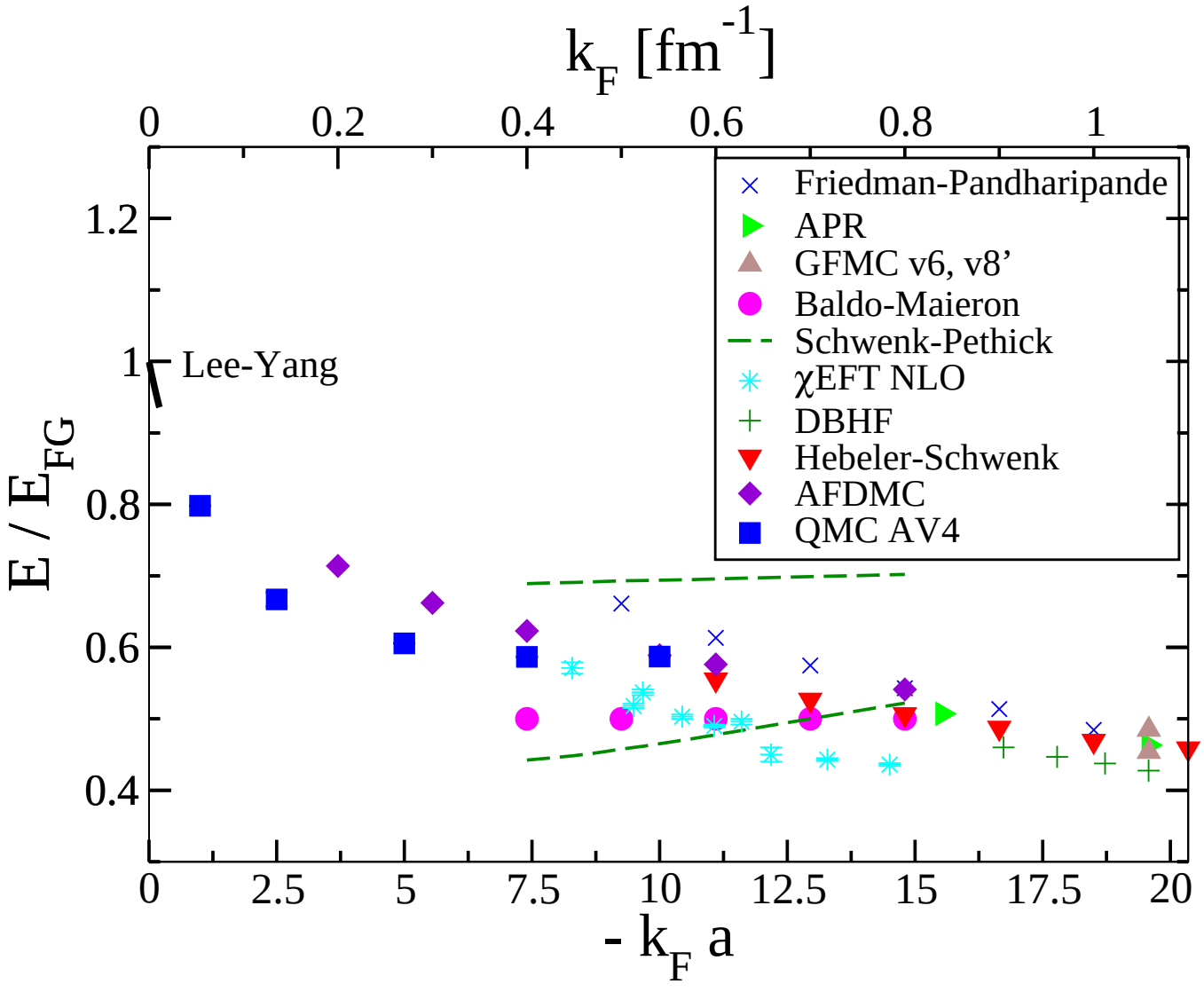

Gezerlis & Carlson, Phys. Rev. C 81, 025803 (2010).

Neutron-matter equation of state at high densities

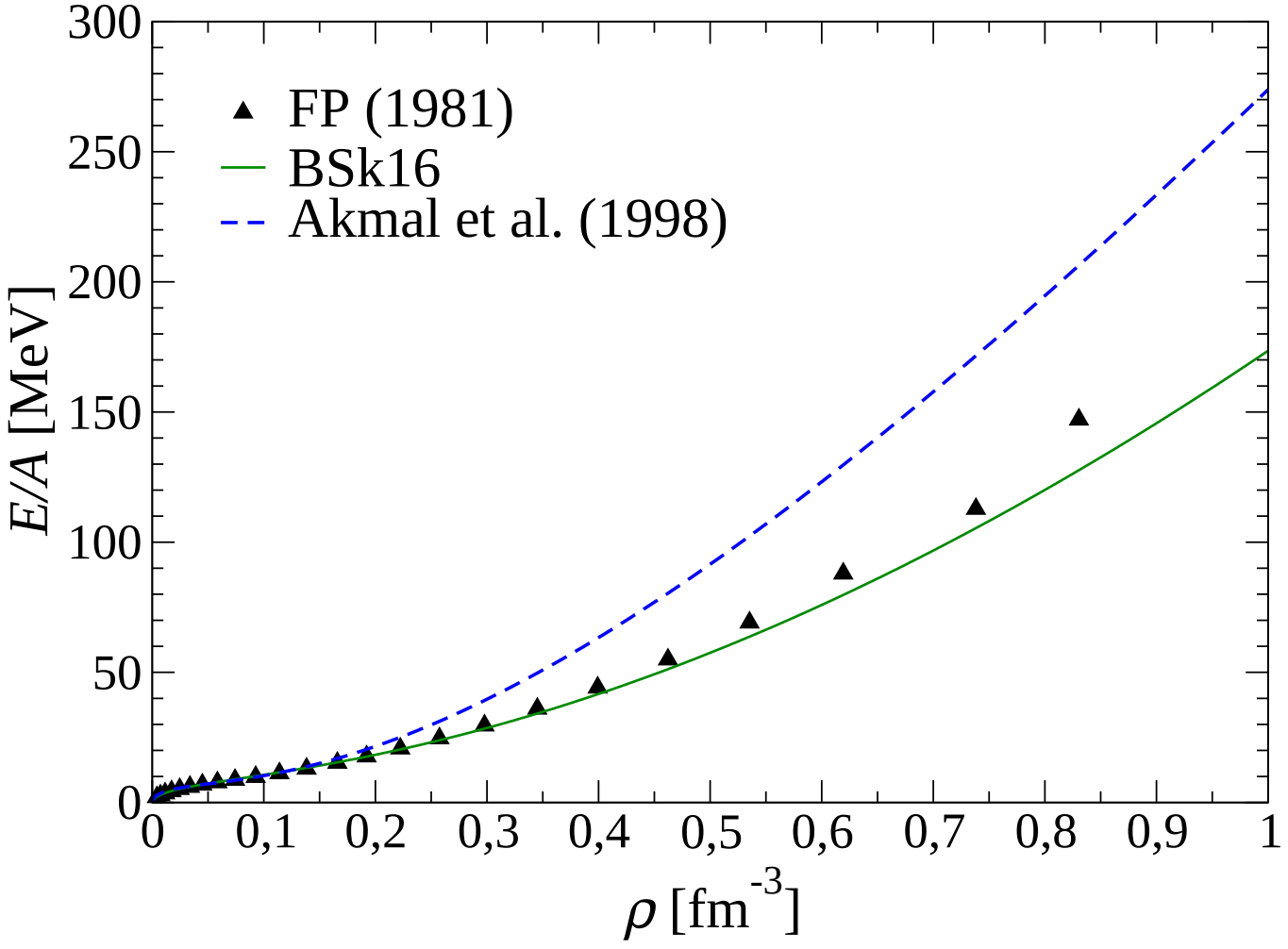

Constraints from heavy-ion collisions

Our functional BSk16 is consistent with the pressure of symmetric nuclear matter inferred from Au+Au collisions

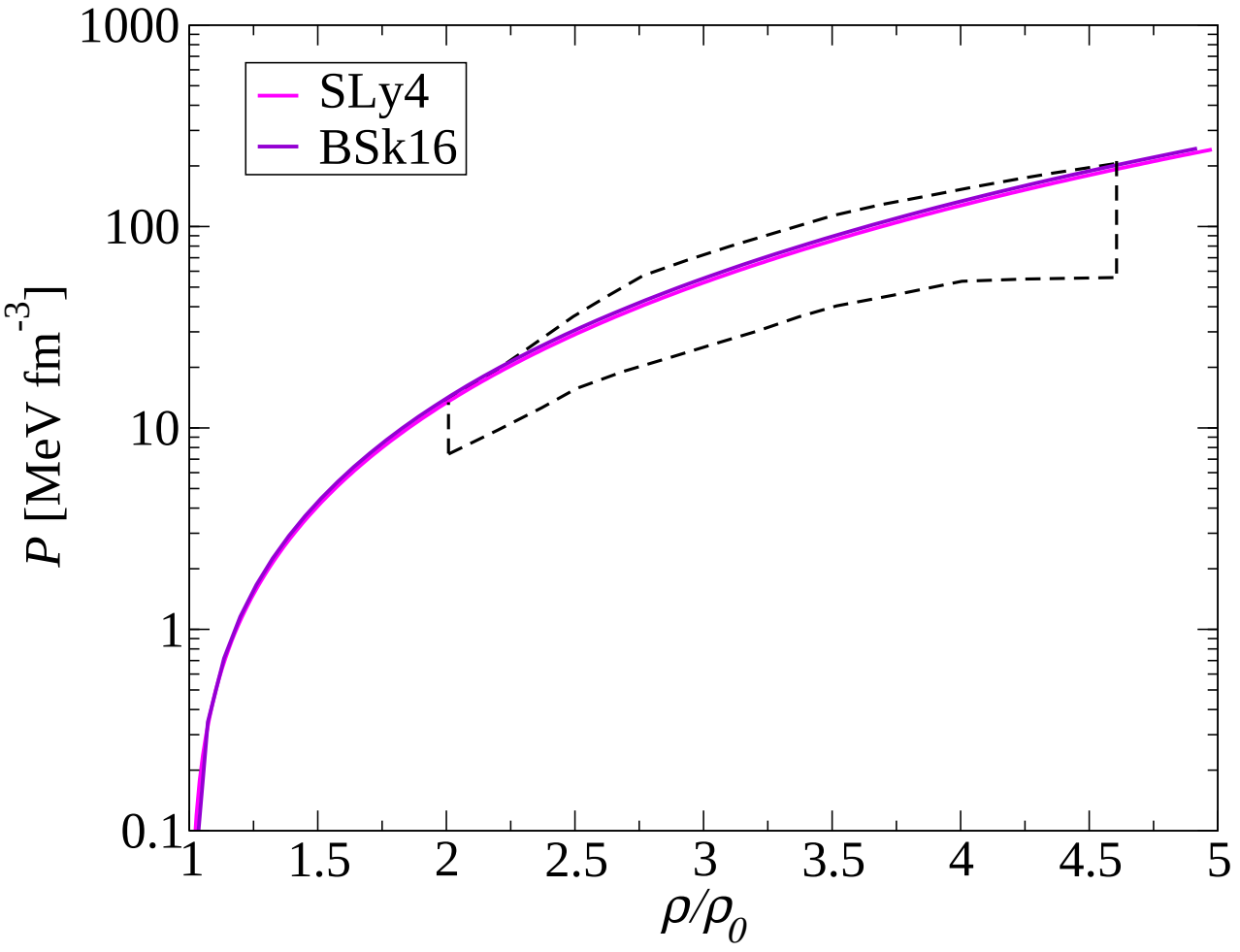

Danielewicz et al., Science 298, 1592 (2002).

HFB-16 mass table

Results of the fit on the 2149 measured masses with $Z, N \geq 8$

	HFB-16	HFB-15	HFB-14	HFB-8
$\sigma(M)$ [MeV]	0.632	0.678	0.729	0.635
$\bar{\epsilon}(M)$ [MeV]	-0.001	0.026	-0.057	0.009
$\sigma(M_{nr})$ [MeV]	0.748	0.809	0.833	0.838
$\bar{\epsilon}(M_{nr})$ [MeV]	0.161	0.173	0.261	-0.025
$\sigma(S_n)$ [MeV]	0.500	0.588	0.640	0.564
$\bar{\epsilon}(S_n)$ [MeV]	-0.012	-0.004	-0.002	0.013
$\sigma(Q_\beta)$ [MeV]	0.559	0.693	0.754	0.704
$\bar{\epsilon}(Q_\beta)$ [MeV]	0.031	0.024	0.008	-0.027
$\sigma(R_c)$ [fm]	0.0313	0.0302	0.0309	0.0275
$\bar{\epsilon}(R_c)$ [fm]	-0.0149	-0.0108	-0.0117	0.0025
$\theta(^{208}\mathrm{Pb})$ [fm]	0.15	0.15	0.16	0.12

HFB-17 mass model: microscopic pairing gaps including medium polarization effects

Fit the $^1S_0$ pairing gaps of both neutron matter and symmetric nuclear matter obtained from **Brueckner calculations taking into account medium polarization effects**

Neutron matter

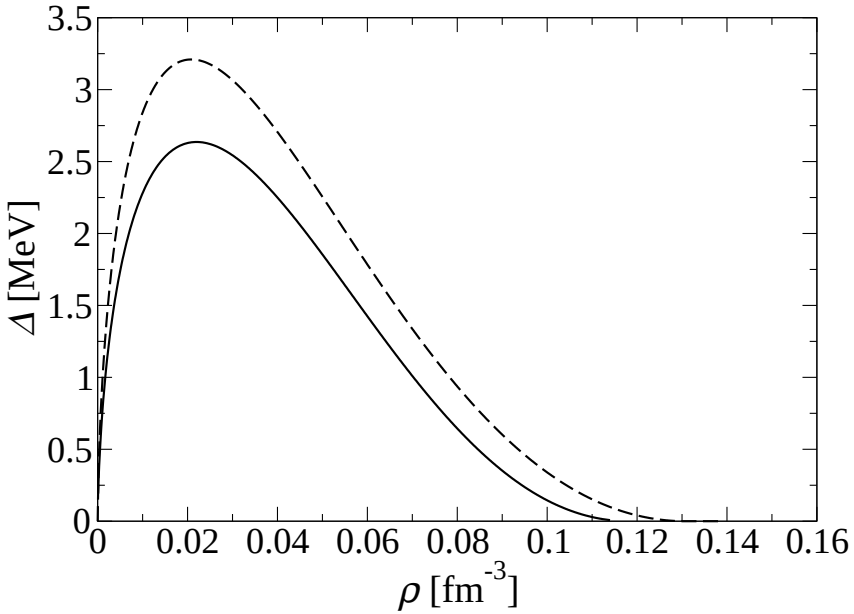

Symmetric nuclear matter

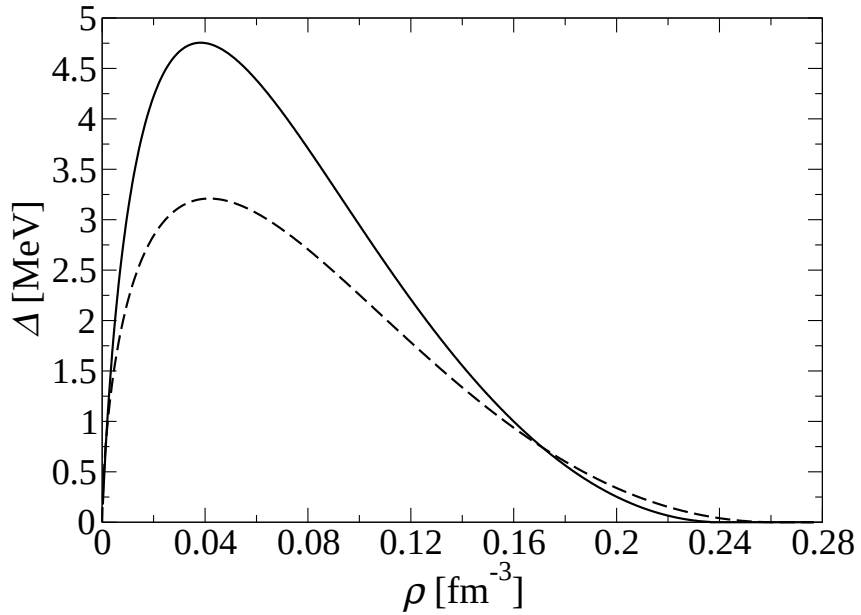

Cao et al.,Phys.Rev.C74,064301(2006).

New expression of the pairing strength

- the pairing strength is allowed to depend on both ρ_n and ρ_p

$$v^{\pi q}[\rho_n, \rho_p] = v^{\pi q}[\Delta_q(\rho_n, \rho_p)]$$

- $\Delta_q(\rho_n, \rho_p)$ is interpolated between that of symmetric matter (SM) and pure neutron matter (NM)

$$\Delta_q(\rho_n, \rho_p) = \Delta_{SM}(\rho)(1 - |\eta|) \pm \Delta_{NM}(\rho_q)\,\eta\,\frac{\rho_q}{\rho}$$

$$\eta = \frac{\rho_n - \rho_p}{\rho_n + \rho_p}$$

- $M_q^* = M$ to be consistent with the neglect of self-energy effects on the gap

Goriely, Chamel, Pearson, PRL102,152503 (2009).

Goriely, Chamel, Pearson, Eur.Phys.J.A42(2009),547.

Density dependence of the pairing strength

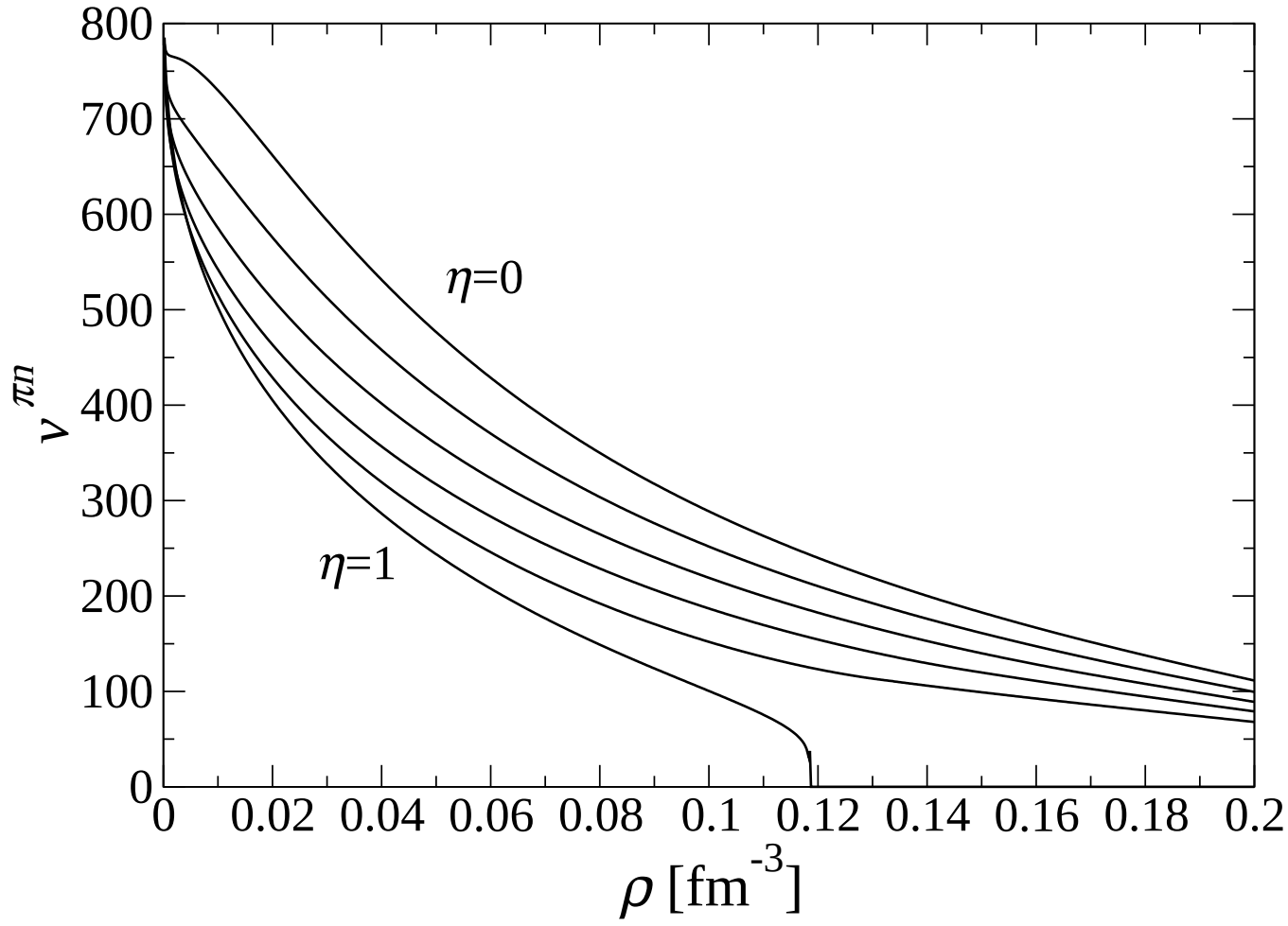

Isospin dependence of the pairing strength

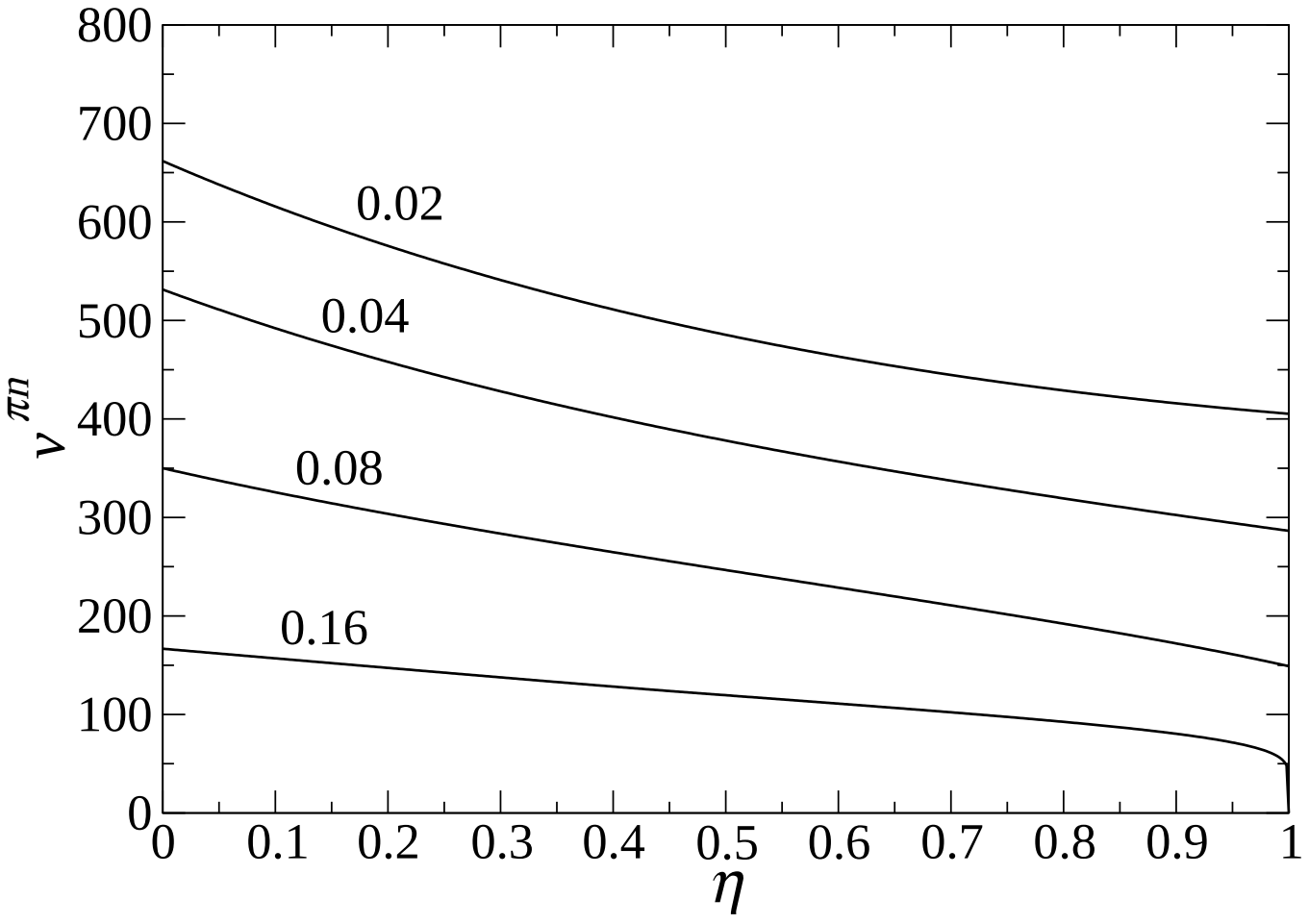

HFB-17 mass table

Results of the fit on the 2149 measured masses with $Z, N \geq 8$

	HFB-16	HFB-17
$\sigma(2149\ M)$	**0.632**	**0.581**
$\bar{\epsilon}(2149\ M)$	-0.001	-0.019
$\sigma(M_{nr})$	0.748	0.729
$\bar{\epsilon}(M_{nr})$	0.161	0.119
$\sigma(S_n)$	0.500	0.506
$\bar{\epsilon}(S_n)$	-0.012	-0.010
$\sigma(Q_\beta)$	0.559	0.583
$\bar{\epsilon}(Q_\beta)$	0.031	0.022
$\sigma(R_c)$	0.0313	0.0300
$\bar{\epsilon}(R_c)$	-0.0149	-0.0114
$\theta(^{208}\mathrm{Pb})$	0.15	0.15

HFB-17 mass predictions

Differences between experimental and calculated masses as a function of the neutron number N for the HFB-17 mass model.

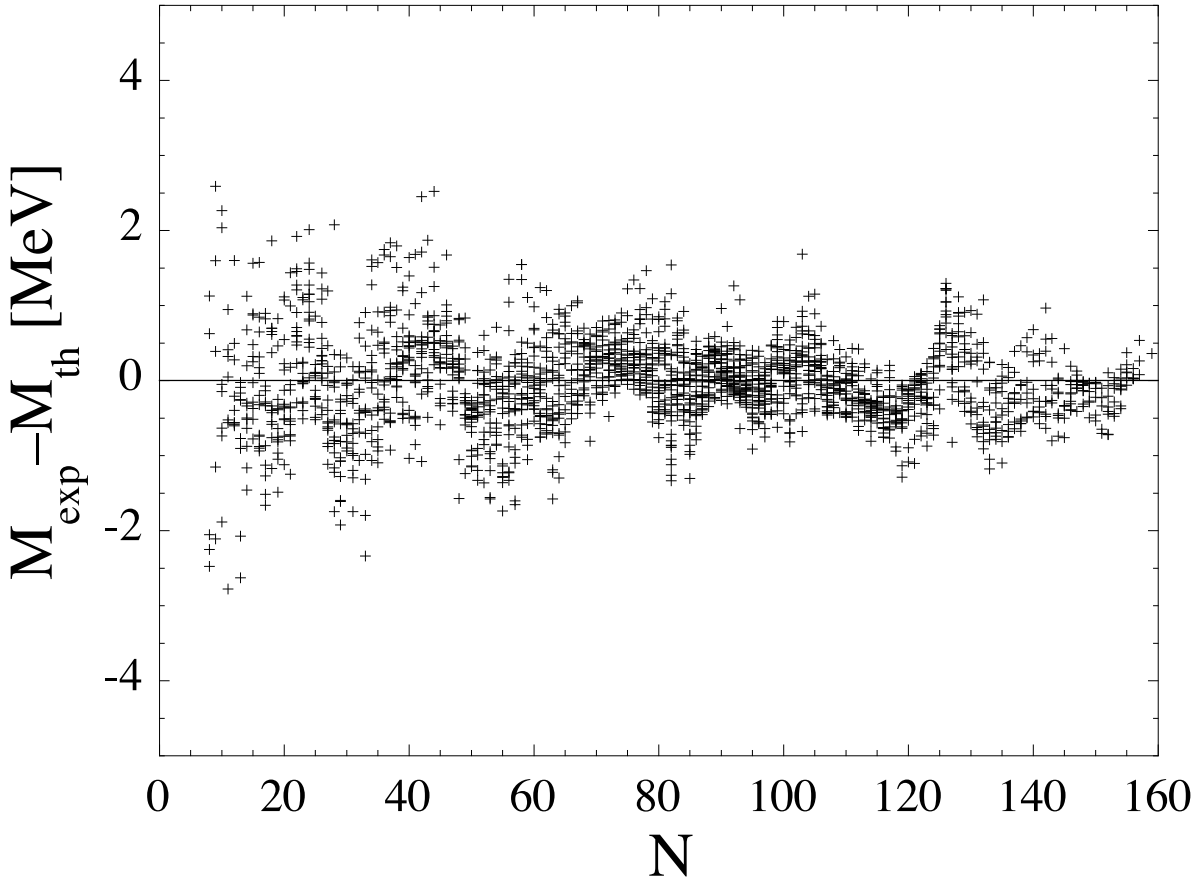

Predictions to newly measured atomic masses

HFB mass models were fitted to the 2003 Atomic Mass Evaluation.

The predictions of these models are in good agreement with new mass measurements

	HFB-16	HFB-17
$\sigma(434\ M)$	0.484	0.363
$\bar{\epsilon}(434\ M)$	-0.136	-0.092
$\sigma(142\ M)$	0.516	0.548
$\bar{\epsilon}(142\ M)$	-0.070	0.172

Litvinov et al., Nucl.Phys.A756, 3(2005)

http://research.jyu.fi/igisol/JYFLTRAP_masses/ gs_masses.txt

Nuclear masses: HFB-16 vs HFB-17

Differences between the HFB-16 and HFB-17 mass predictions as a function N for all $8 \leq Z \leq 110$ nuclei lying between the proton and neutron drip lines.

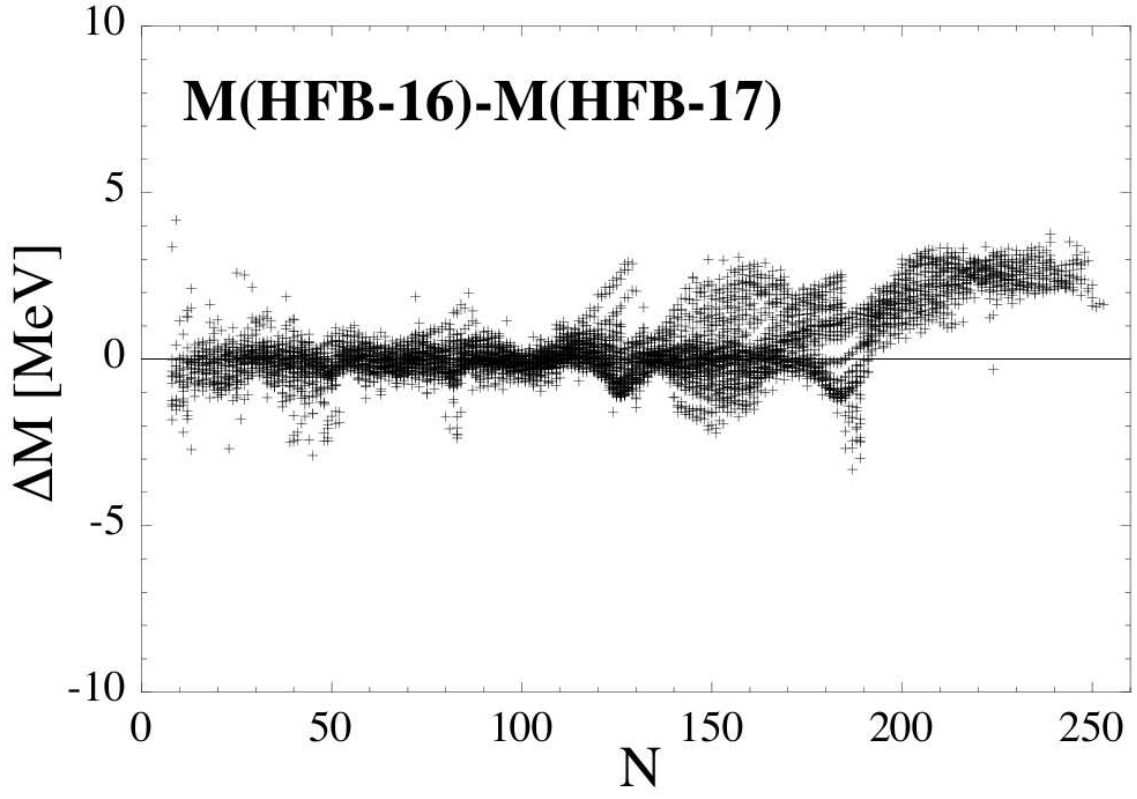

Superfluidity in neutron-star crusts with the Wigner-Seitz approximation

The HFB equations in neutron-star crusts have been already solved by several groups using the W-S approximation

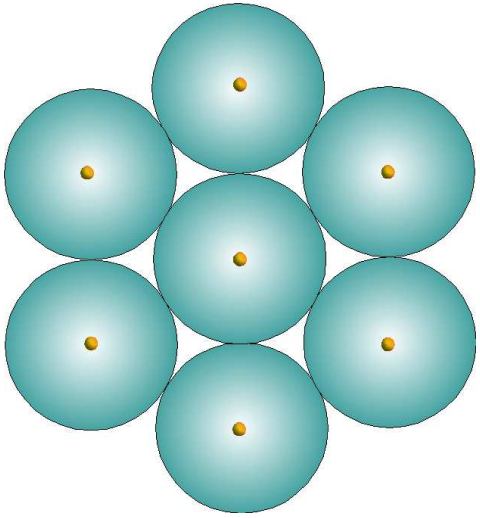

The effects of the clusters are found to be dramatic at high densities ($\gtrsim$ 0.03 nucleons per fm^3), in some cases the pairing gaps are almost completely suppressed

Baldo et al., Eur.Phys.J. A 32, 97(2007).

Limitations of the W-S approximation

Problems

- the results of HFB calculations **depend on the boundary conditions** which are not unique
- the nucleon densities and pairing fields exhibit **spurious fluctuations** due to box-size effects

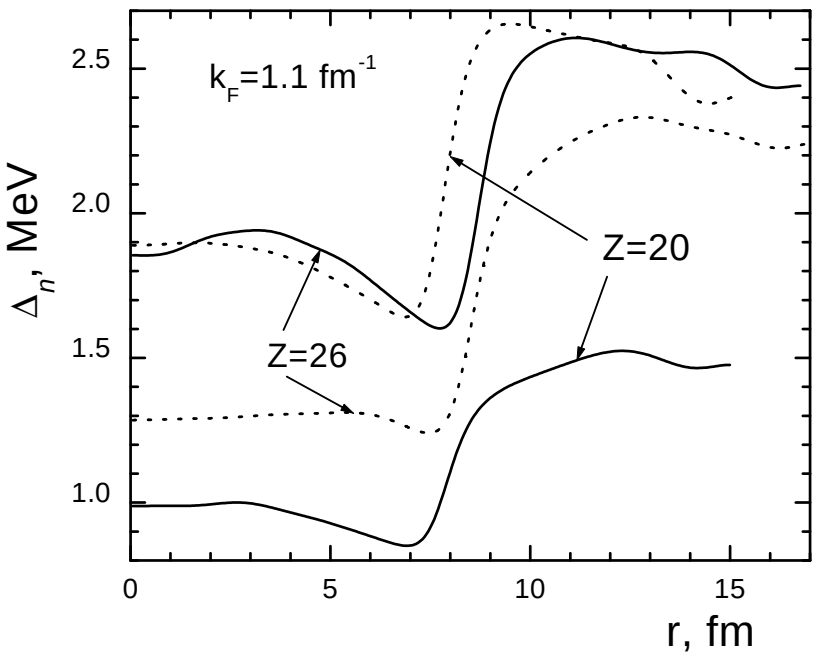

Spurious shell effects $\propto 1/R^2$ are very large in the bottom layers of the crust and are enhanced by the self-consistency of the calculations.

Baldo et al., Eur.Phys.J. A 32, 97(2007).

Nuclear band theory

Solution

Go beyond the W-S app. by using the band theory of solids
Chamel et al., Phys.Rev.C75(2007)055806.

The band theory takes consistently into account both nuclear clusters and free neutrons

$$\varphi_{\alpha \boldsymbol{k}}(\boldsymbol{r}) = e^{\mathrm{i}\boldsymbol{k}\cdot\boldsymbol{r}} u_{\alpha \boldsymbol{k}}(\boldsymbol{r})$$

$$u_{\alpha \boldsymbol{k}}(\boldsymbol{r} + \boldsymbol{T}) = u_{\alpha \boldsymbol{k}}(\boldsymbol{r})$$

- $\alpha \rightarrow$ rotational symmetry around the lattice sites
- $\boldsymbol{k} \rightarrow$ translational symmetry of the crystal

Anisotropic multi-band neutron superfluidity

In the decoupling approximation, the Hartree-Fock-Bogoliubov equations reduce to the BCS equations

$$\Delta_{\alpha\boldsymbol{k}} = -\frac{1}{2}\sum_{\beta}\sum_{\boldsymbol{k}'} \bar{v}^{\mathrm{pair}}_{\alpha\boldsymbol{k}\alpha-\boldsymbol{k}\beta\boldsymbol{k}'\beta-\boldsymbol{k}'} \frac{\Delta_{\beta\boldsymbol{k}'}}{E_{\beta\boldsymbol{k}'}} \tanh\frac{E_{\beta\boldsymbol{k}'}}{2T}$$

$$\bar{v}^{\mathrm{pair}}_{\alpha\boldsymbol{k}\alpha-\boldsymbol{k}\beta\boldsymbol{k}'\beta-\boldsymbol{k}'} = \int \mathrm{d}^3r\, v^{\pi}[\rho_n(\boldsymbol{r}),\rho_p(\boldsymbol{r})]\,|\varphi_{\alpha\boldsymbol{k}}(\boldsymbol{r})|^2|\varphi_{\beta\boldsymbol{k}'}(\boldsymbol{r})|^2$$

$$E_{\alpha\boldsymbol{k}} = \sqrt{(\varepsilon_{\alpha\boldsymbol{k}}-\mu)^2+\Delta^2_{\alpha\boldsymbol{k}}}$$

$\varepsilon_{\alpha\boldsymbol{k}}$, μ and $\varphi_{\alpha\boldsymbol{k}}(\boldsymbol{r})$ are obtained from band structure calculations

Chamel et al., Phys.Rev.C81,045804 (2010).

Validity of the decoupling approximation

The decoupling approximation means that

$$\int \mathrm{d}^3\boldsymbol{r}\, \varphi^*_{\alpha\boldsymbol{k}}(\boldsymbol{r})\Delta(\boldsymbol{r})\varphi_{\beta\boldsymbol{k}}(\boldsymbol{r}) \simeq \delta_{\alpha\beta} \int \mathrm{d}^3\boldsymbol{r}\, |\varphi_{\alpha\boldsymbol{k}}(\boldsymbol{r})|^2\Delta(\boldsymbol{r})$$

This approximation is justified whenever $\Delta(\boldsymbol{r})$ varies slowly as compared to $\varphi_{\alpha\boldsymbol{k}}(\boldsymbol{r})$ for those states in the vicinity the Fermi level.

- bad for weakly bound nuclei (delocalized continuum states involved while $\Delta_q(\boldsymbol{r})$ drop to zero outside nuclei)
- good for strongly bound nuclei
- exact for uniform matter

$\Rightarrow$ reasonable for dense layers of neutron-star crusts

Analogy with terrestrial multi-band superconductors

Multi-band superconductors were first studied by Suhl et al. in 1959 but clear evidence were found only in 2001 with the discovery of MgB_2 (two-band superconductor)

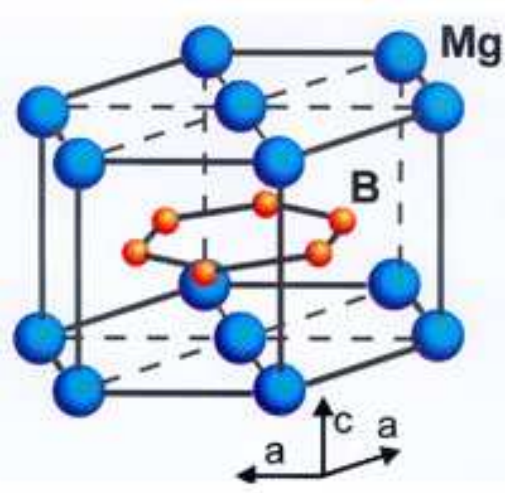

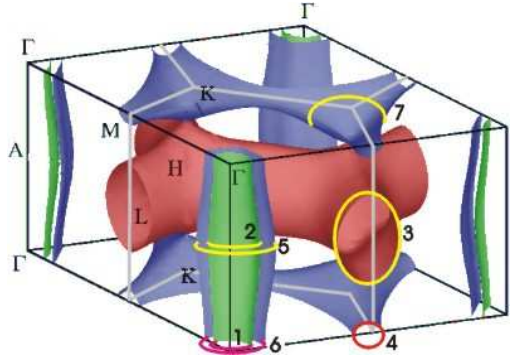

In neutron-star crusts,

- the number of bands can be huge $\sim$ up to a thousand!
- both intra- and inter-band couplings must be taken into account

Description of neutron star crust beyond neutron drip

The equilibrium structure of the inner crust is determined with the Extended Thomas-Fermi (up to 4th order)+Strutinsky Integral method (ETFSI).

- Pairing is expected to have a small impact on the composition and is therefore neglected.
- Nuclei are assumed to be spherical.

Onsi et al., Phys.Rev.C77,065805 (2008).

Advantages of ETFSI method

- very fast approximation to the full Hartree-Fock method
- avoids the difficulties related to boundary conditions but include proton shell effects (neutron shell effects are generally much smaller and are therefore omitted) *Chamel et al.,Phys.Rev.C75(2007),055806.*

Ground-state composition of the inner crust

Results for BSk14

n_b (fm^{-3})	Z	A
0.0003	50	200
0.001	50	460
0.005	50	1140
0.01	40	1215
0.02	40	1485
0.03	40	1590
0.04	40	1610
0.05	20	800
0.06	20	780

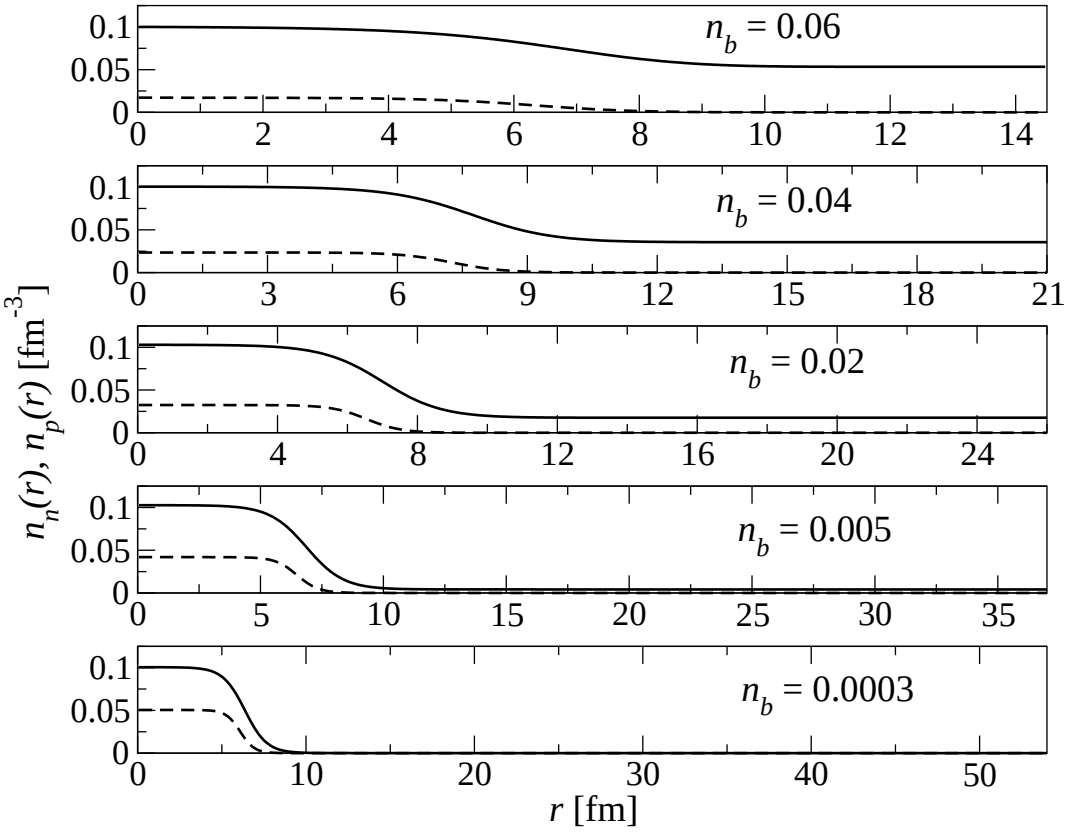

Onsi, Dutta, Chatri, Goriely, Chamel and Pearson, Phys.Rev.C77,065805 (2008).

Ground-state composition of the inner crust

ETFSI calculations for two different functionals

with HFB-14

n_b (fm^{-3})	Z	A
0.0003	50	200
0.001	50	460
0.005	50	1140
0.01	40	1215
0.02	40	1485
0.03	40	1590
0.04	40	1610
0.05	20	800
0.06	20	780

with HFB-17

n_b (fm^{-3})	Z	A
0.0003	50	190
0.001	50	432
0.005	50	1022
0.01	50	1314
0.02	40	1258
0.03	40	1334
0.04	40	1354
0.05	40	1344
0.06	40	1308

Neutron pairing gaps vs single-particle energies

Example at $n_b = 0.06$ fm^{-3} with BSk16

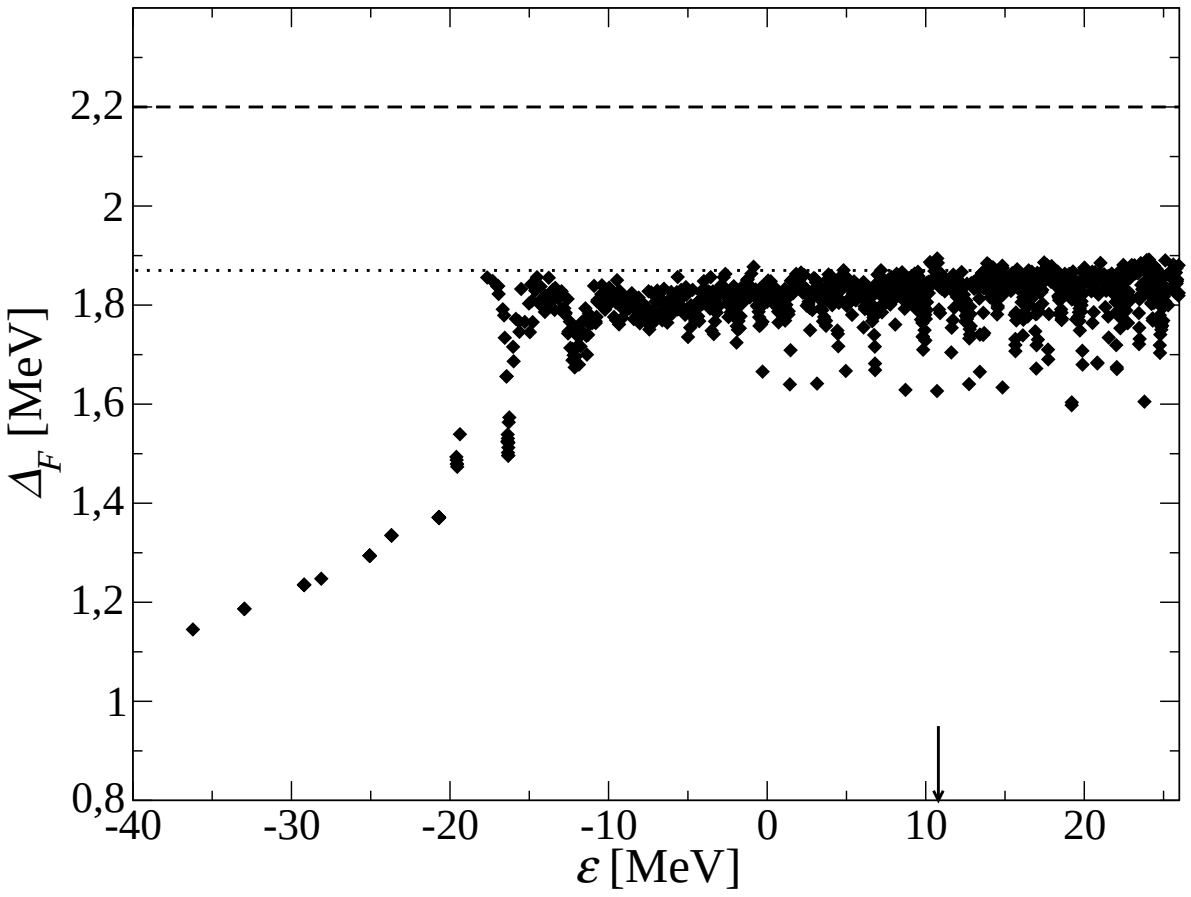

The presence of clusters reduces $\Delta_{\alpha \boldsymbol{k}}$ but much less than predicted by previous calculations

Average neutron pairing gap vs temperature

Example at $n_b = 0.06$ fm^{-3} with BSk16

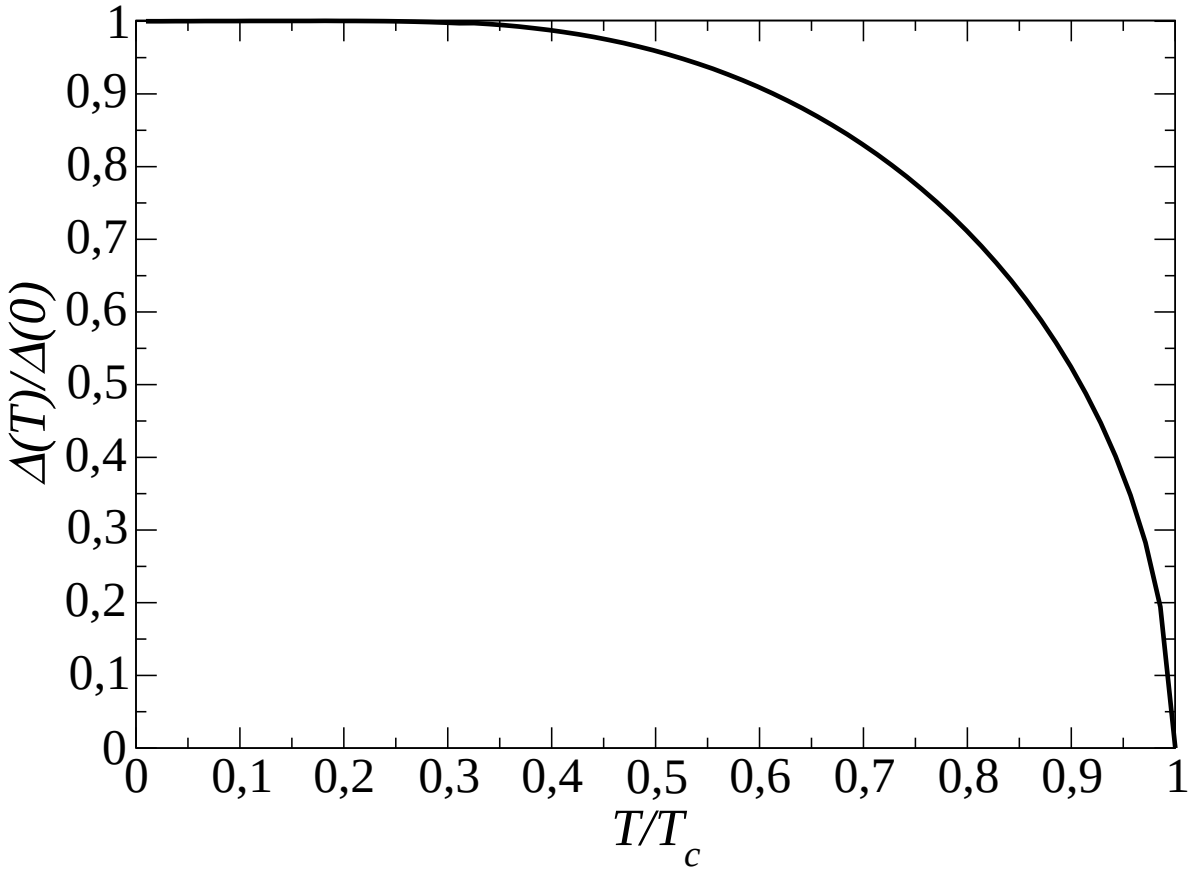

- $\Delta_{\alpha \boldsymbol{k}}(T)/\Delta_{\alpha \boldsymbol{k}}(0)$ is a universal function of T
- The critical temperature is approximately given by the usual BCS relation $T_c \simeq 0.567 \Delta_F$

Neutron pairing gaps vs density

n_n^f is the density of unbound neutrons
$\Delta_{\rm u}$ is the gap in neutron matter at density n_n^f
$\bar{\Delta}_{\rm u}$ is the gap in neutron matter at density n_n

n_b [fm^{-3}]	Z	A	n_n^f [fm^{-3}]	$\Delta_{\rm F}$ [MeV]	$\Delta_{\rm u}$ [MeV]	$\bar{\Delta}_{\rm u}$ [MeV]
0.07	40	1218	0.060	1.44	1.79	1.43
0.065	40	1264	0.056	1.65	1.99	1.65
0.06	40	1260	0.051	1.86	2.20	1.87
0.055	40	1254	0.047	2.08	2.40	2.10
0.05	40	1264	0.043	2.29	2.59	2.33

- the nuclear clusters lower the gap by $10-20\%$
- both bound and unbound neutrons contribute to the gap

Pairing field and local density approximation

The effects of inhomogeneities on neutron superfluidity can be directly seen in the pairing field

$$\Delta_n(\boldsymbol{r}) = -\frac{1}{2} v^{\pi n}[\rho_n(\boldsymbol{r}), \rho_p(\boldsymbol{r})]\tilde{\rho}_n(\boldsymbol{r}), \;\; \tilde{\rho}_n(\boldsymbol{r}) = \sum_{\alpha,\boldsymbol{k}}^{\Lambda} |\varphi_{\alpha\boldsymbol{k}}(\boldsymbol{r})|^2 \frac{\Delta_{\alpha\boldsymbol{k}}}{E_{\alpha\boldsymbol{k}}}$$

Neutron pairing field for $n_b = 0.06$ fm^{-3} at $T = 0$

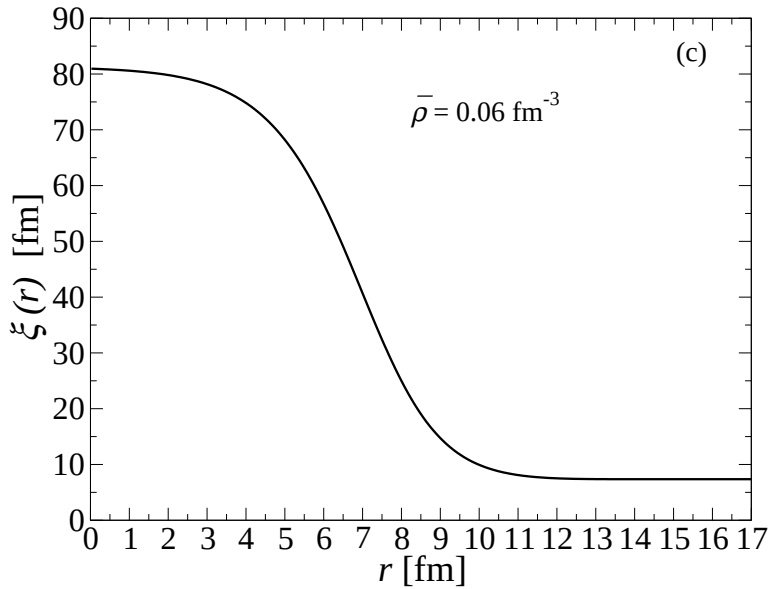

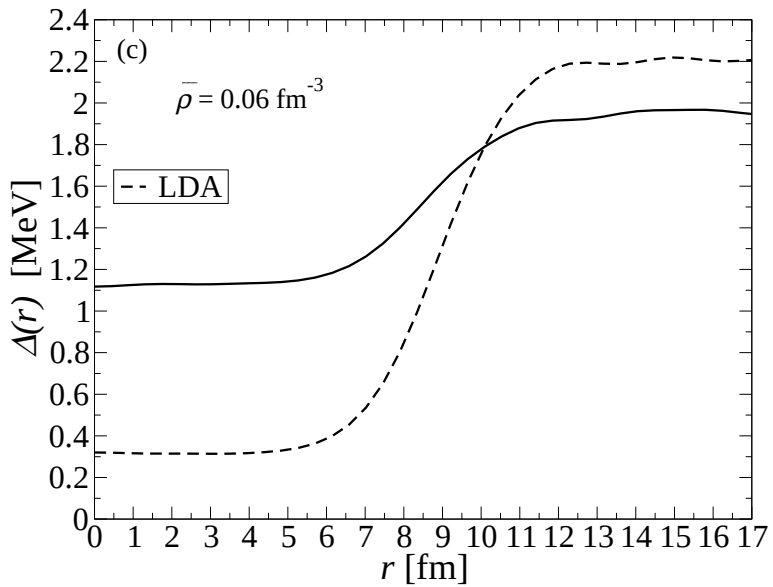

Chamel et al., Phys.Rev.C81(2010)045804.

Pairing field at finite temperature

At $T > 0$, the neutron pairing field is given by

$$\Delta_n(\boldsymbol{r}) = -\frac{1}{2} v^{\pi n}[\rho_n(\boldsymbol{r}), \rho_p(\boldsymbol{r})]\tilde{\rho}_n(\boldsymbol{r}), \quad \tilde{\rho}_n(\boldsymbol{r}) = \sum_{\alpha,\boldsymbol{k}}^{\Lambda} |\varphi_{\alpha\boldsymbol{k}}(\boldsymbol{r})|^2 \frac{\Delta_{\alpha\boldsymbol{k}}}{E_{\alpha\boldsymbol{k}}} \tanh \frac{E_{\alpha\boldsymbol{k}}}{2T}$$

Neutron pairing field for $n_b = 0.06$ fm^{-3}

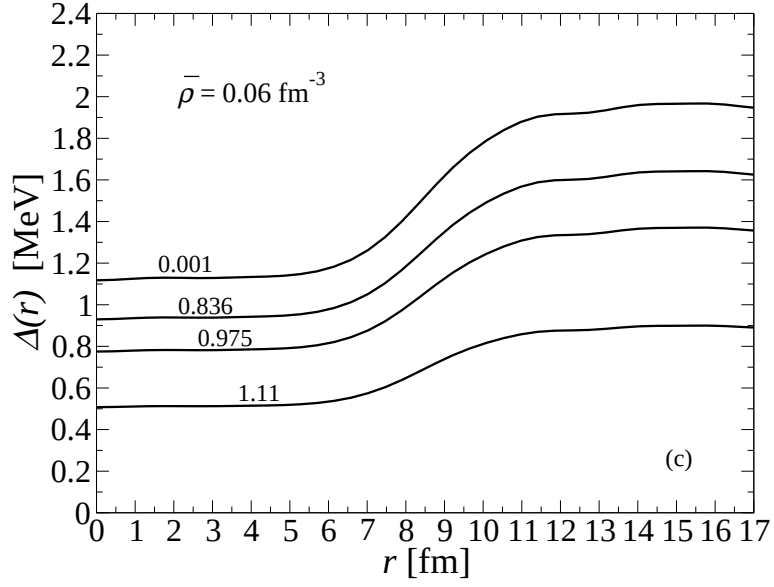

The superfluid becomes more and more homogeneous as T approaches T_c

Chamel et al., Phys.Rev.C81(2010)045804.

Impact of the pairing cutoff

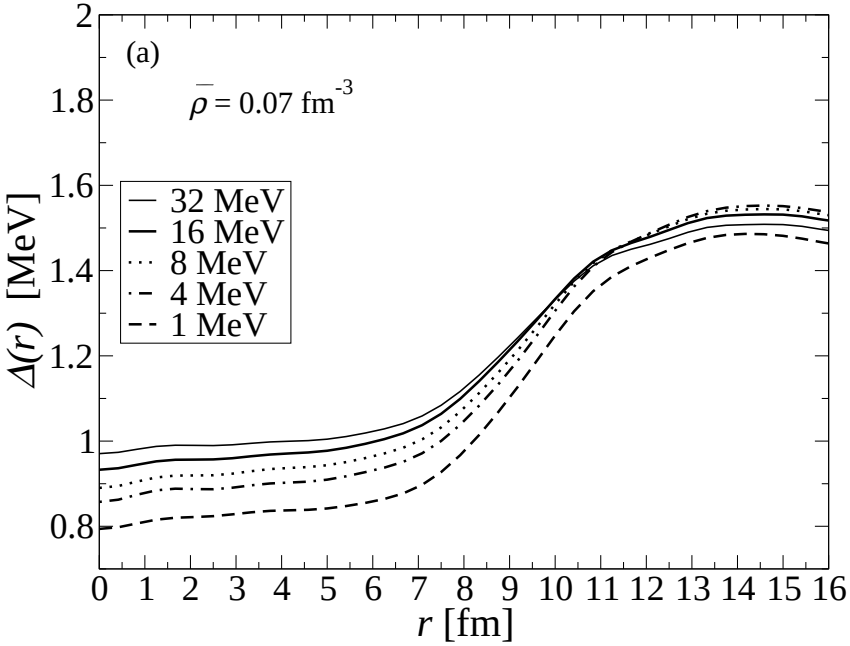

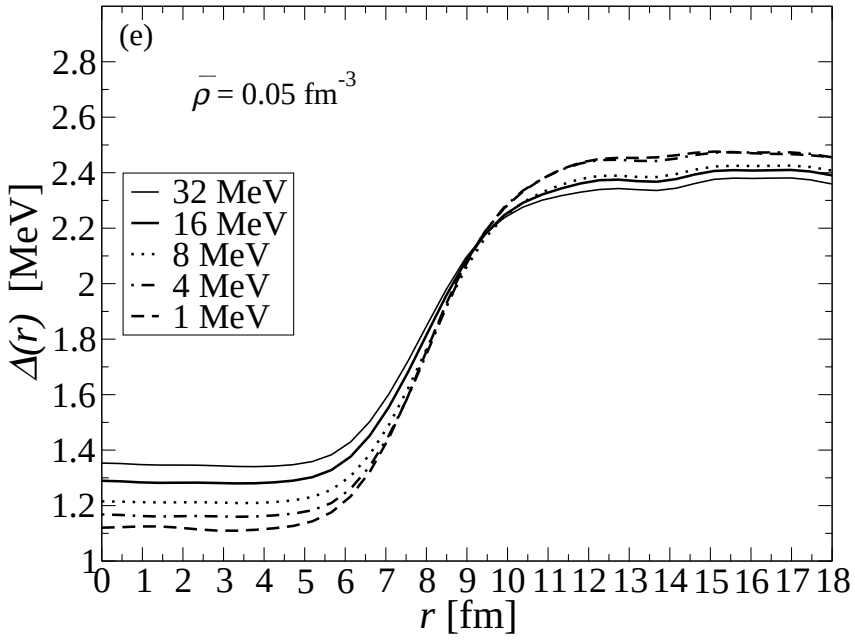

n_b [fm^{-3}]	$\Delta_{F0}(16)$ [MeV]	$\Delta_{F0}(8)$	$\Delta_{F0}(4)$	$\Delta_{F0}(2)$	$\Delta_{F0}(1)$
0.070	1.39	1.38	1.37	1.36	1.29
0.050	2.27	2.25	2.27	2.26	2.24

Pairing gaps (hence also critical temperatures) are very weakly dependent on the pairing cutoff.

Impact on thermodynamic quantities : specific heat

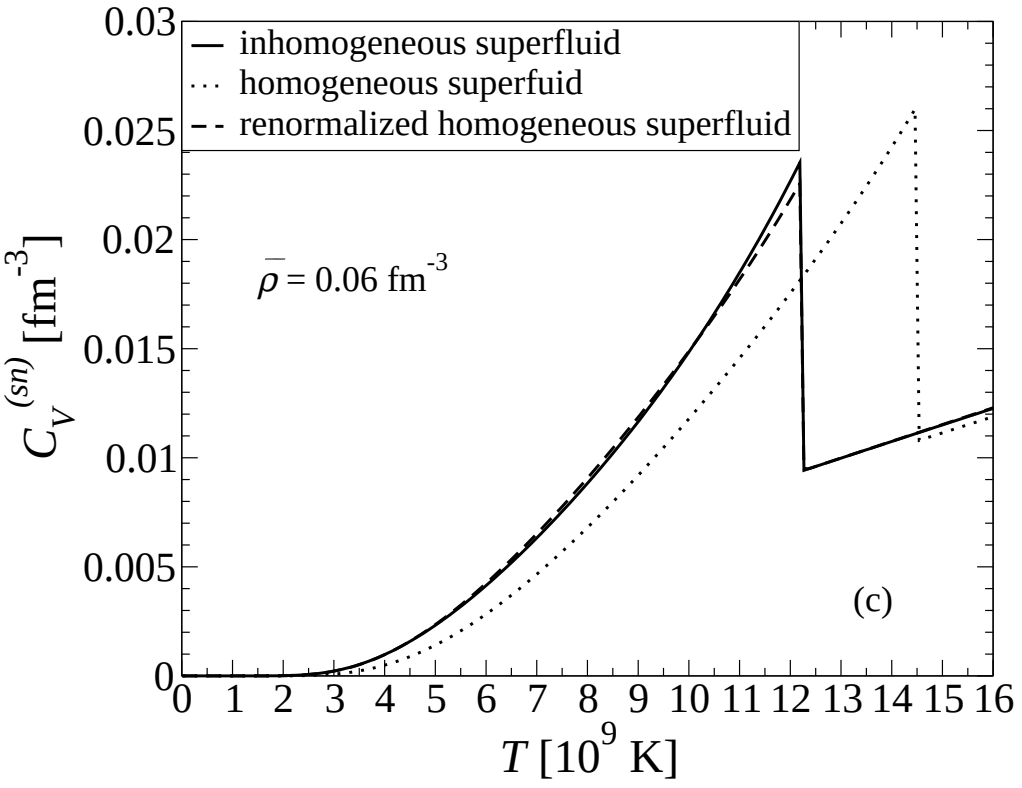

- Band structure effects are small. This remains true for non-superfluid neutrons.
  Chamel et al, Phys. Rev. C 79, 012801(R) (2009)
- The renormalization of T_c comes from the density dependence of the pairing strength.

How “free” are neutrons in neutron-star crusts?

Due to the interactions with the periodic lattice, neutrons move in the inner crust as if they had an **effective mass** $m_n^\star$.

This is a well-known effect in solid-state physics (typically $m_e^\star \sim 1 - 2m_e$).

$m_e^\star$ is related to the current-current correlation function.

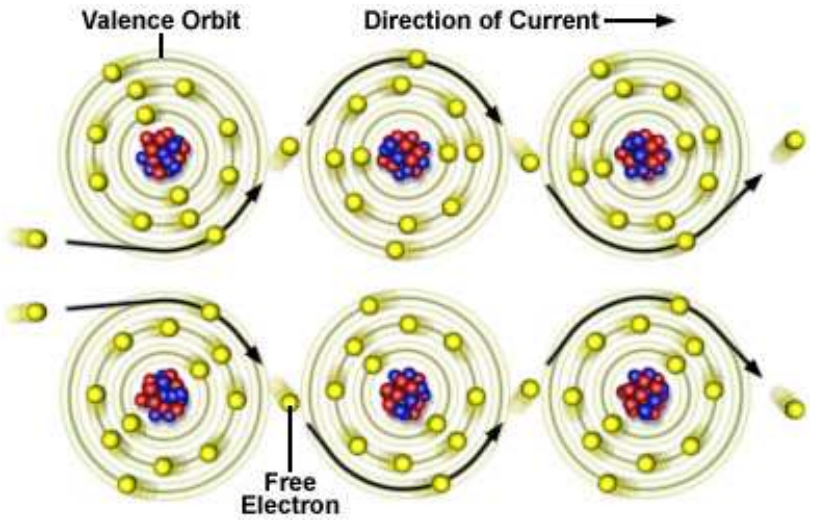

This entrainment effect is very important for the **hydrodynamics of the neutron superfluid**.

Carter, Chamel, Haensel, Int.J.Mod.Phys.D15(2006)777.

Pethick, Chamel, Reddy, Prog.Theor.Phys.Sup.186(2010)9.

Unbound neutrons vs conduction neutrons

n_n^f is the **density of unbound neutrons**
$n_n^c = n_n^f m_n / m_n^\star$ is the **density of conduction neutrons**

n_b (fm^{-3})	Z	A	n_n^f/n_n (%)	n_n^c/n_n^f (%)
0.0003	50	200	20.0	82.6
0.001	50	460	68.6	27.3
0.005	50	1140	86.4	17.5
0.01	40	1210	88.9	15.5
0.02	40	1480	90.3	7.37
0.03	40	1595	91.4	7.33
0.04	40	1610	88.8	10.6
0.05	20	800	91.4	30.0
0.06	20	765	91.5	45.9
0.07	20	714	92.0	64.6
0.08	20	665	104	64.8

Entrainment effects in cold atoms

Simiar entrainment effects are also predicted in unitary Fermi gases and could thus be **potentially measured in laboratory**.
Example: unitary Fermi gas in a 1D optical lattice

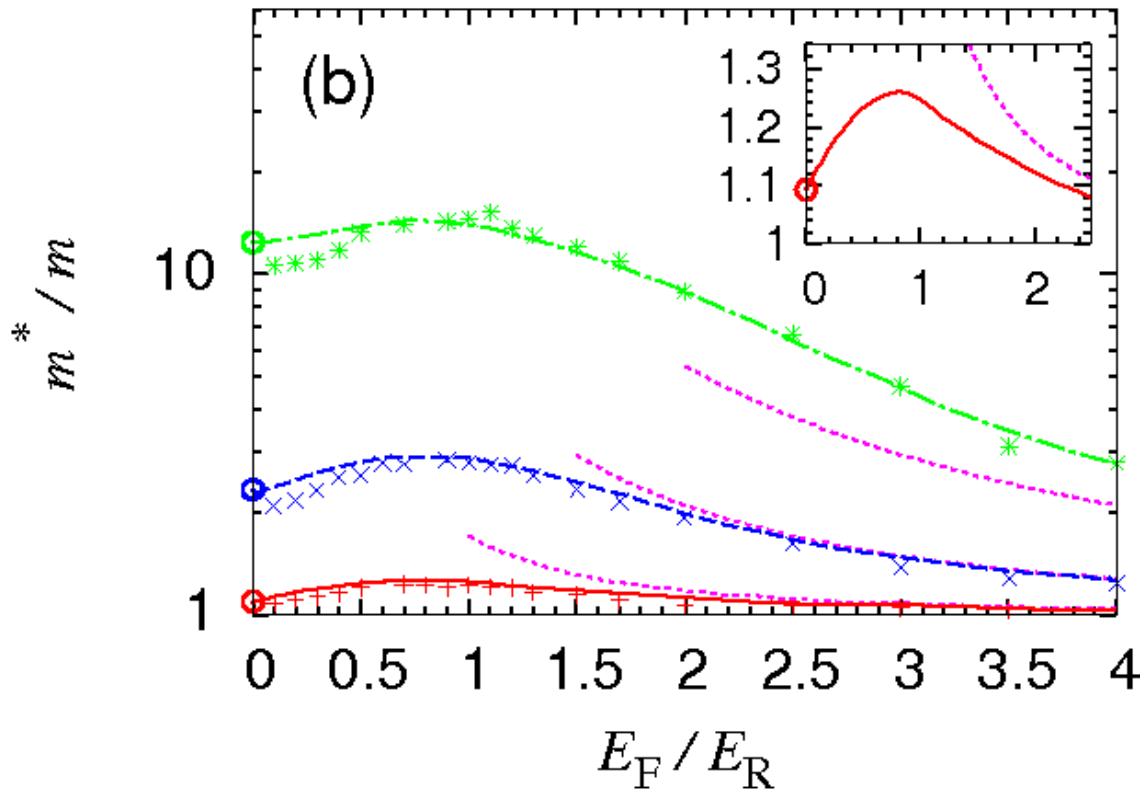

Watanabe et al., Phys. Rev. A78(2008),063619

Summary

1. The nuclear energy density functional (EDF) theory allows for a consistent treatment of superfluid neutrons in neutron-star crusts.
2. We have developed semi-local EDF constrained by experiments and N-body calculations:
   - they give an excellent fit to essentially all nuclear mass data ($\sigma = 581$ keV for HFB-17)
   - they reproduce various properties of infinite nuclear matter (EoS, pairing gaps, *etc*)
3. Using the band theory of solids, we have shown that the nuclear lattice affects both the static and the dynamic properties of the neutron superfluid in the dense layers of neutron-star crusts.